



NTNU – Trondheim
Norwegian University of
Science and Technology

Assessment of ultrasonic assisted drilling

Noralf Vedvik

Subsea Technology

Submission date: June 2015

Supervisor: Olav Egeland, IPK

Co-supervisor: Sigbjørn Sangesland, IPT

Norwegian University of Science and Technology
Department of Production and Quality Engineering


Preface

This thesis is delivered upon the end of my master's degree in Subsea Technology at the Norwegian University of Science and Technology, department of Production and Quality Engineering. With the specialization topic of manufacturing technology. The project itself was conducted at the department of Petroleum Engineering and Applied Geophysics, during spring 2015.

Force, stick-slip and wear test were performed at SINTEF Petroleum Research.

The ideas to this project were a combination of guidance from my supervisor, Sigbjørn Sangesland, and ideas that came up during the specialization project last fall.

Trondheim, 10.06.2015



Noralf Vedvik

Acknowledgement

Firstly I would like to give thanks to my supervisor Sigbjørn Sangesland who gave me the opportunity to conduct this thesis. He has been a great support during my work.

A great thanks is given to the engineers at the department of Petroleum Engineering and Applied Geophysics. Åge Siverson have been of great help with the electrical circuit board and lending me equipment from his laboratory. Håkon Myhren has done a great job with producing the equipment I designed for the test.

I'm grateful for SINTEF Petroleum Research being so generous to lend me their equipment and laboratory. The employees at SINTEF and especially Hans Lund, Jørn Stenebråten and Mohammad Bhuiyan for being so co-operative and helpful.

A special thanks to my good friends Emil Valaker, Ida Bueide and Mikkel Kristiansen. Emil for helping me with the microscope pictures, Ida and Mikkel for proofreading my report. I would also like to thank all my friends at the university for a good time together, keeping the spirit up.

N.V

Summary

This thesis investigates the potential of using ultrasonic assisted drilling (UAD) in the oil and gas industry in order to increase drilling performance. UAD has shown positive effects when drilling in materials like metal and ceramics. A dedicated tool for introducing ultrasonic vibration into a standard TerraTek scratch test machine were designed and manufactured. The conducted experiments investigated the effect of ultrasonic vibration with regard to normal and shear force, stick-slip effect and wear. The main results from the experiments were:

- The force readings from all the experiments shows that ultrasonic vibration has a positive effect on drilling performance in rock samples. Tests performed at Berea sandstone shows 40% and 90% reduction in shear force and normal force respectively.
- The lack of being able to reproduce any real stick-slips in the tests makes it difficult to draw a conclusion if the ultrasonic vibration has any effect on stick-slip.
- The wear test indicates that the ultrasonic vibration has a negative impact in terms of wear on the cutter. More work needs to be done to clarify if this is a problem using Polycrystalline diamond compact (PDC) bits.

In the end, a design was presented as a solution for integration of a piezoelectric actuator into a wireline deployed well tractor, used for drilling scale in production wells.

In general, the results from the force tests were positive and further work should be performed. Further work should include analysis of increased amplitude of PDC cutter, wear on the PDC cutter, and the effect of introducing a full size bit with ultrasonic vibration for scale milling.

Sammendrag

Denne oppgaven undersøker potensialet for bruk av ultrasonisk assistert boring (UAD) i olje- og gassindustrien for å øke boreytelsen. UAD har vist positiv effekt ved boring i materialer som metall og keramikk. Det ble konstruert og produsert et dedikert verktøy for å tilføre ultrasoniske vibrasjoner til en standard TerraTek skrape maskin. Forsøkene undersøkte effekten av ultrasoniske vibrasjoner med hensyn til normal og skjærkraft, stick-slip effekt og slitasje. Hovedresultatene fra forsøkene var:

- Kraftavlesningene fra alle forsøkene viser at ultrasoniske vibrasjoner har en positiv effekt på borekraften i steinprøver. Tester utført på Berea-sandsten viser en reduksjon på henholdsvis 40% og 90% av skjærkraft og normalkraft.
- Siden det ikke lot seg gjøre å reprodusere "stick-slips" i testen er det vanskelig å trekke en konklusjon om hvorvidt ultrasonisk vibrasjon har noen effekt på "stick-slips".
- Slitasje-testen indikerer at ultrasonisk vibrasjon har en negativ effekt i form av slitasje på kutteren. Mer arbeid må gjøres for å avklare om dette er et problem på Polycrystalline diamond compact (PDC) kuttere.

Til slutt blir det presentert en løsning for integrering av en piezoelektrisk aktuator til en wireline brønntraktor, til boring av avleiringer produksjonsbrønner.

Generelt var resultatene fra kraftavlesningene positive og videre arbeid bør utføres. Videre arbeid bør omfatte analyse av økt amplitude på PDC-kutter, slitasje på PDC-kutter, og effekten av å bruke en fullskala borekrone med ultrasonisk vibrasjon for boring av avleiringer i produksjonsbrønner.

Table of Contents

Preface.....	i
Acknowledgement.....	ii
Summary	iii
Sammendrag	iv
1 Introduction	1
2 Theory	3
2.1 Ultrasonic Assisted Drilling	3
2.1.1 Force Reduction by Vibration.....	3
2.1.2 Vibration Effect on Wear.....	3
2.1.3 Stick slip.....	5
2.2 Well Tractor	6
2.3 Piezoelectric Actuator.....	7
2.3.1 Designing Piezoelectric Actuators.....	8
2.4 Scale.....	11
3 Experimental work.....	13
3.1 Original Rig.....	13
3.2 Extra Features.....	14
3.2.1 Force Reduction by Vibration.....	14
3.2.2 Stick-Slip Reduction by Vibration	14
3.2.3 Vibration Effect on Wear.....	17
3.3 Experimental Setup	18
4 Results.....	19
4.1 Experimental Results	19
4.1.1 Force Reduction by Vibration.....	20
4.1.2 Stick-Slip Reduction by Vibration	25
4.1.3 Vibration Effect on Wear.....	25
4.2 Ultrasonic Assisted Tractor Operation	29
4.2.1 Electrical	29
4.2.2 Pressure Equalization	30
4.2.3 Motor.....	31
4.2.4 Gear	31
4.2.5 Actuator.....	33
4.2.6 Drill Bit.....	38

5	Discussion.....	39
5.1	Force Reduction by Vibration	39
5.2	Stick-Slip reduction by Vibration	39
5.3	Vibration Effect on Wear	39
5.4	Ultrasonic Assisted Tractor Operation	40
6	Conclusion.....	41
7	Proposed Further Work	43
8	Nomenclature	45
9	References	47
	Appendix A, Technical Drawings	1
	Appendix B, Electric Circuit board.....	13
	Appendix C, Wireline.....	15
	Appendix D, Springs	17
	Appendix E, Piezoelectric Actuator	21
	Appendix F, LabView Program	23
	Appendix G, 3D Pictures.....	25

1 Introduction

In the later years, the demand for better and more effective methods of drilling and cutting of materials have increased, leading to further development of Ultrasonic Assisted Drilling (UAD).

In the oil and gas industry, drilling and well interventions are time consuming and expensive. Typical day rates are in the order of \$400 000 for semi-submersible drilling rigs. Well interventions reduce or stop production, leading to lost income. By increasing drilling efficiency, large savings can be made.

Very little research has been done with regard to UAD in rock, National Aeronautics and Space Administration (NASA) has developed a core sampler for use on the Mars rover. This core sampler uses only ultrasonic vibration to drill, with no rotation (Bar-Cohen, Sherrit, and Bao 2007).

To get a deeper understanding in how ultrasonic vibration affects rock-drilling performance, a series of experiments are conducted. The experiments measure the cutting force, stick-slip effect and wear on the cutter.

At the end, a proposed solution for integrating a piezoelectric element into well a tractor is presented. Well tractors have limited power supply and can increase its range by increasing the efficiency. The well tractor with vibration is intended for scale removal.

The first section is a literature survey on existing technologies using UAD.

2 Theory

The use of ultrasonic vibration in different manufacturing processes is well documented for more than 60 years, and was first technically described in the 1940s by Lewis Balamuth (Edelen 2007). The first ultrasonic drilling machines developed, was without rotation. In 1964 Ultrasonic assisted drilling (UAD) was invented by Legge (Ishikawa et al. 1998).

This chapter will go thru today's technology. Describe some of the effects ultrasonic vibration has in other applications and how it can effect drilling using a well tractor. In the end an introduction to well tractors, piezoelectric actuators and scale in production tubing will be given.

2.1 Ultrasonic Assisted Drilling

UAD is a hybrid process combining conventional drilling and ultrasonic oscillation. Applicable to both ductile and brittle materials. (Chang and Bone 2005). Experiments with calcium aluminum silicate and magnesia stabilized zirconia have shown that the material removal rates obtained from UAD is six to ten times higher than that from a conventional drilling process under similar conditions (Prabhakar 1992). In comparison with conventional drilling, UAD show for superior surface finish and low tool pressure (Cleave 1976).

2.1.1 Force Reduction by Vibration

Force reduction is especially interesting in regard to the well tractor, due to limited power supply through the wireline. By reducing the power needed to turn the drill bit and the power needed to push the tractor, it will be possible to perform deeper operations or do the operations faster.

Experiences from UAD on other materials than rock has shown some good tendencies when it comes to force reduction.

Pujana et al. (2009), made an analysis of ultrasonic-assisted drilling of Ti6Al4V. By introducing ultrasonic vibration with 9 μ m amplitude, they observed a reduction from 350N during conventional drilling, to 170N with UAD.

Ishikawa et al. (1998), presented a study on combined vibration drilling by ultrasonic and low frequency vibrations for hard and brittle materials. The result of this study showed that by inducing both ultrasonic and low frequency vibrations to the workpiece, the lowest cutting force, tool wear and nicest cut were obtained. However, applying two different vibrations to a drill bit is complicated, and applying just ultrasonic vibration is by far the second best alternative. Reducing drilling force from 14N to 7N.

2.1.2 Vibration Effect on Wear

Wear on the drill bit, is an important factor. Rapid wear means more tripping of equipment out and into the well. Resulting in increased time spent on operation, loss of production time plus day rate of service/drilling vessel (Ford 2012).

How UAV will affect the drill bit is an important question. UAV have shown varying effects on cutting tools, depending on cutting material.

Tsuboi et al. (2012), studied the effect of Ultrasonic vibration and cavitation-aided micromachining of hard and brittle materials. When drilling through silicon carbide they experienced a remarkable increase in the number of holes each drill bit lasted by introducing axial vibration to the bit. By conventional drilling, a drill bit lasted 12 holes, and with vibration, it lasted 40.

Azarhoushang and Akbari (2006), performed an experimental investigation of ultrasonic assisted drilling of Inconel 738-LC. Inconel is in the range of new alloys that causes high tool temperatures and rapid wear of cutting edges. By introducing vibration to the drilling, they experienced a significantly decrease in tool wear, shown in Figure 2.1. In addition, they experienced up to 60% improvement in surface roughness and circularity on the machined pieces.

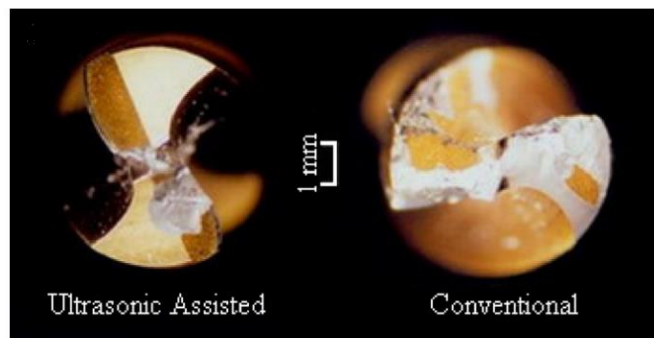


Figure 2.1: Worn TiN-coated drill bits (Azarhoushang and Akbari 2006).

Chang and Bone (2005), focused on burr size reduction in drilling by ultrasonic assistance. Their work focused on drilling in A1100-0 aluminum. Their research pointed out a significant reduction in burr width and height. They observed an increase in wear on the HSS drill bits in form of chipping on UAD compared to conventional drilling. However, TiN-coated HSS drill bits did not show any signs of chipping.

2.1.3 Stick slip

Stick-slip as it is known in drilling situations can occur throughout the drill string for many reasons, the most prevalent form of stick-slip and the form that is relevant for UAD, occur at the drill bit and is referred to as bit related stick-slip. Figure 2.2 illustrates a stick-slip. Stick-slip is initiated when the energy or torque being delivered to the bit by the drill string is not sufficient to overcome the formation being drilled, at this point the bit slows down or stops in the “stick” phase. The torque builds up in the drill string resulting in twists until enough torque has been developed to crush the formation, at which point the drill bit breaks free from the “stick” phase and rapidly accelerates, rotating at several times the intended rotary speed (Deen, Wedel, and Nayan 2011, Wedel, Mathison, and Hightower 2011).

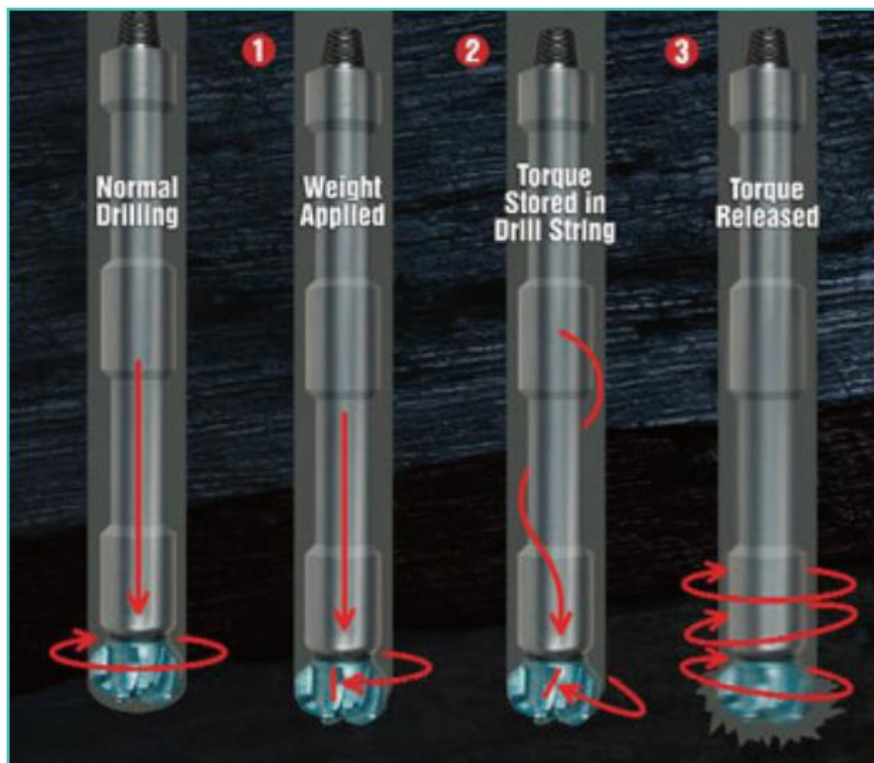


Figure 2.2: Illustration of stick slip(Deen, Wedel, and Nayan 2011).

Stick-slip can severely shorten a Polycrystalline diamond compact (PDC) cutters life (Figure 2.3), resulting in poor runs. Damage to expensive equipment is not limited to the drill bit. Downhole motors or rotary steerable systems, measurement tools, stabilizers, drill collars, and drill pipe are all string components that can be damaged by stick-slip(Wedel, Mathison, and Hightower 2011, Chen, Blackwood, and Lamine 2002).



Figure 2.3: Bit wear without and with stick slip failure(Deen, Wedel, and Nayan 2011).

Stick-slip also effects drilling by well tractor. Power supplied by tractor/motor combination is limited. As a result, the system must be optimized to deliver a regular supply of power to the drill bit. This can be difficult as downhole conditions can be hard to read and indications of stalling can be missed (Oiltools 2014).

2.2 Well Tractor

The Well Tractor (Figure 2.4) is an auxiliary tool used to push well Intervention equipment along highly deviated and horizontal sections of oil or gas wells. Without the tractor, well interventions in wells like this must be done with a drill string, requiring a much bigger and more expensive vessel. Normally a motor is mounted on the end of the tractor; this is used to power the milling and cleaning tools that are mounted on to the shaft. Wireline well tractors can only be used for drilling as long as there is flow in the well, to get rid of cuttings.



Figure 2.4: Illustration of well tractor without drill bit(AkerSolutions 2013).

Power to the well tractor and tools are limited by the power that can be delivered through the wireline. For example a well tractor in a well using the wireline in Appendix C and assuming $P=3\text{kW}$ as max input:

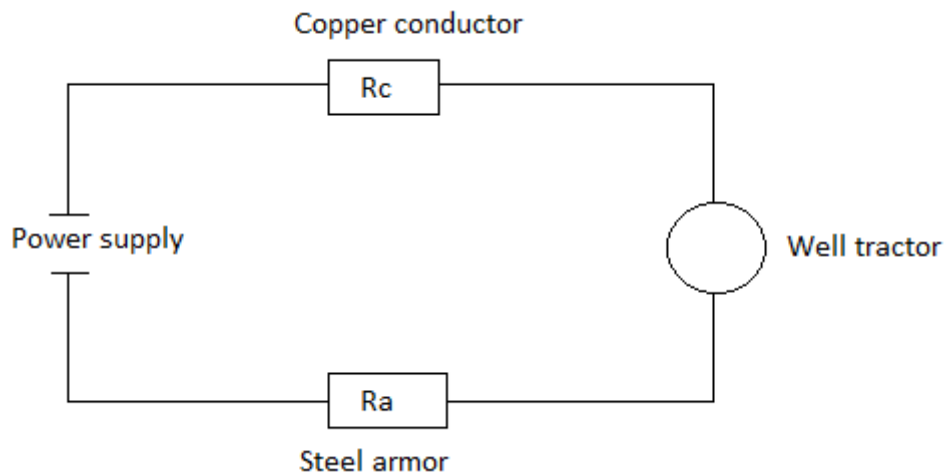


Figure 2.5: Wire diagram for well tractor.

Loss through wireline shown in Figure 2.5:

$$U=1000\text{V, max low voltage (NORSOK 2001)}$$

$$I=3000\text{W}/1000\text{V}= 3\text{A}$$

$$R_c= 6,6\Omega/\text{km} \quad R_a=3,94\Omega/\text{km}$$

$$R= (6,6+3,94)\Omega/\text{km} =10,54\Omega/\text{km}$$

$$U_{\text{LOST}}= 10,54\Omega/\text{km} \cdot 3\text{A}=31,62\text{V}/\text{km}$$

$$P_{\text{LOST}}= 31,62\text{V}/\text{km} \cdot 3\text{A}=94,86\text{W}/\text{km}$$

This results in the well tractor in the bottom of the deepest oil wells, reaching up to 10km, to have lost almost 1kW of the power available. This will also be more critical as wells are being drilled in deeper waters.

2.3 Piezoelectric Actuator

In 1880, the Curie brothers first examined the piezoelectric effect on crystal materials, which has the capacity to produce electrical charges in response to externally applied forces, called the direct effect. This effect is reciprocal, meaning that the piezoelectric material changes its dimensions under applied electrical charges(Technologies 2012).

A piezoelectric material has electromechanical interaction between its mechanical and electrical state. When a piezoelectric material is compressed, it creates an electrical field, as shown in Figure 2.6. The inverse is also true. When a piezoelectric material is subjected to an electric field, it will change dimensions(M4Siences 2011).

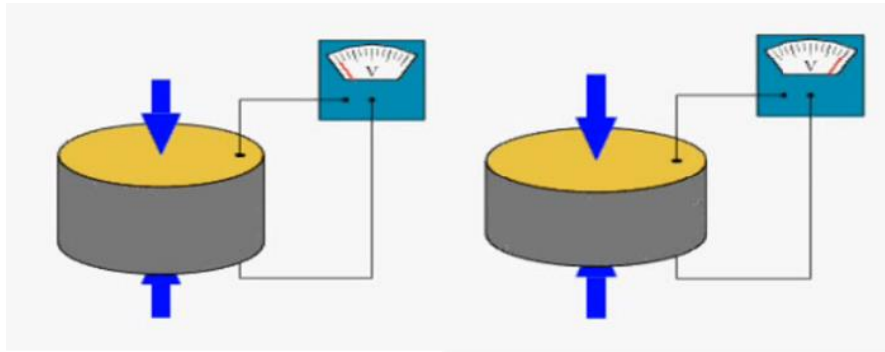


Figure 2.6: Piezoelectric, low compression on the left, high compression on the right.

Much has happened since 1880. In 1988, Multilayer Actuators (MLAs) were introduced to the market. This circumvented many of the earlier limitations of the piezo actuator. MLAs are easy to operate, and are being increasingly used in various applications. The required excitation voltage of 150V or less is well adapted to modern electronics, compared to over 1000V on earlier actuators (Technologies 2012). MLAs are individual slices of piezoelectric materials that can be connected, forming a piezo stack (Figure 2.7).

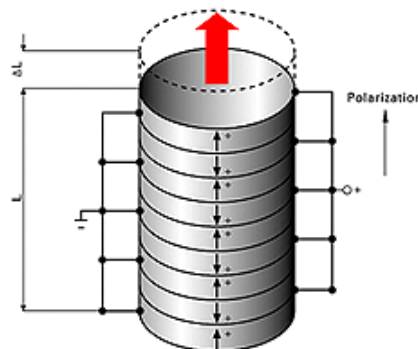


Figure 2.7: Piezo stack (PI 2014).

2.3.1 Designing Piezoelectric Actuators

How to design piezoelectric actuators is a large topic, only the most essential factors for the actuator described in section 4.2 will be presented. Information about the design process is gathered from Noliac (2014), Instrumente (2001), Instrumente (2015) and Technology (2015).

For Lead Zirconate Titanate (PZT) materials a strain on the order of 1/1000 (0.1%) can be achieved with high reliability. This means that a 100 mm long PZT actuator can expand by 100 micrometers when the maximum electric field is applied. If both the regular and inverse electric fields are used, a relative strain up to 0.2 % is achievable.

Piezoelectric actuators are sensitive to pulling and shear forces. In addition, the piezoelectric elements can get depolarized:

- Electrical depolarization; exposure to a strong electrical field of opposite polarity to the polarization field will depolarize a piezoelectric element.
- Mechanical depolarization; mechanical depolarization occurs when the mechanical stress on a piezoelectric element becomes sufficiently high to disturb the domain orientation and hence destroy the alignment of dipoles.
- Thermal depolarization; if a piezoelectric element is heated to its Curie point, the polarization direction becomes disordered and the elements becomes completely depolarized.

PZT ceramics can withstand high pushing forces and carry loads of several tons. PZT ceramic material can withstand pressures up to approximately 250 MPa ($2500 \times 10^5 \text{N/m}^2$) before it breaks mechanically. For practical applications, this value must not be approached. Depolarization occurs at pressures around 20 to 30 % of the mechanical limit. If the maximum compressive force for a PZT is exceeded, damage to the ceramics as well as depolarization may occur.

In the next sub chapters, the most important formulas for calculations of piezoelectric actuators are presented.

Actuator Stiffness

The actuator stiffness k_{PZT} is an important parameter for calculating force generation, resonant frequency, and system behavior.

$$k_{PZT} = \frac{E \cdot A}{l}$$

Where:

E = Young's modulus for the PZT compound (Pa)

A = Cross section area of the actuator (m^2)

l = Actuator length (m)

Force generation

Blocked force, is the maximum force the actuator can produce.

$$F_{max} \approx k_{PZT} \cdot \Delta L_0$$

Where:

k_{PZT} = PZT actuator stiffness (N/m)

ΔL_0 = Max. nominal displacement without external force (m)

Reduction in displacement

Components installed on or working against the actuator will reduce the displacement.

Constant force:

A mass is installed on the PZT which applies a force $F = m \cdot a$. The zero point will be offset by an amount of:

$$\Delta L_N \approx \frac{F}{k_{PZT}}$$

Where:

ΔL_N = Zero point offset (m)

F = Force (mass times gravity) (N)

k_{PZT} = PZT actuator stiffness (N/m)

Changing force:

When working against springs the external force changes, reducing the displacement of the PZT. Maximum displacement loss:

$$\Delta L_R = \Delta L_0 \times \left(1 - \frac{k_{PZT}}{k_{PZT} + k_{spring}}\right)$$

Where:

ΔL_0 = Max. nominal displacement without external force (m)

ΔL_R = Lost displacement due to external spring (m)

k_{PZT} = PZT actuator stiffness (N/m)

k_{spring} = Spring stiffness (N/m)

Resonant Frequency

Maximum operating frequency for the actuator, limited by the extra weight added to the actuator.

$$f_0 = 1/2 \pi \cdot \sqrt{\frac{k_{PZT}}{m_{eff}}}$$

Where:

f_0 = Resonant frequency (Hz)

k_{PZT} = PZT actuator stiffness (N/m)

m_{eff} = Effective mass (kg)

$$m_{eff} \approx \frac{m_{PZT}}{3} + m$$

m_{PZT} = Weight of the actuator(kg)

m = Mass of end pieces (weight that the actuator need to push) (kg)

Electrical Requirements

Average power requirement from the actuator.

$$P_a \approx C \cdot U_{max} \cdot U_{p-p} \cdot f$$

Where

P_a = Average power (W)

f = Operating frequency

U_{p-p} = Peak-peak drive voltage (V)

U_{max} =Maximum output voltage swing of the amplifier (V)

C = PZT actuator capacitance (F)

$$C = n \cdot \epsilon_{33} \cdot A/d_s$$

n = number of layers

ϵ_{33} = Relative dielectric constant (no dimension)

A = Cross section area of the actuator (m²)

d_s = Layer thickness (m)

2.4 Scale

Scale is a major issue in the oil and gas industry. Under certain conditions, the natural chemistry of produced fluid derived from the reservoir geology can lead to the formation of salts, which in turn can deposit as scale in the production system. Similarly, deposition can be promoted when seawater either is injected into the reservoir to maintain pressure or has migrated to the producing zone from another zone. A scale build up like in Figure 2.8 can appear within 24 hours, ruining the productivity of a well. Inhibitors are used to avoid scale, using too little or wrong mix of inhibitor may lead to scale. When scale first is present, well intervention is required. Scale, depending on its composition can be very hard to remove (Crabtree et al. 1999, BP 2010). For this project, scale is compared with drilling through sandstone.



Figure 2.8: Scale build up in 3-inch pipe (BP 2010).

3 Experimental work

The goal of the experiment is to measure and examine the forces acting on the Polycrystalline Diamond Compact (PDC) bits while drilling. Moreover, see what effect ultrasonic frequency vibration has on the cutter. Adding a stick-slip effect mechanism to the rig opens for the possibility to test the effect with ultrasonic vibration.

3.1 Original Rig

The original test rig is a TerraTek 7060-200 (Figure 3.1). The original rig is built for scratch testing of rock samples, but without vibration and stick-slip mechanism. The rig works in the following way: The unit performing the measurements on the cutting tool, hereby called the measurement unit, is stationary. The rock sample is placed on the lower rig. The lower rig moves the rock sample with a typical speed of 4mm/s and a maximum force of 4000N towards the cutting tool. The movement of the rig is quite similar to the movement of one tooth on a PDC bit.

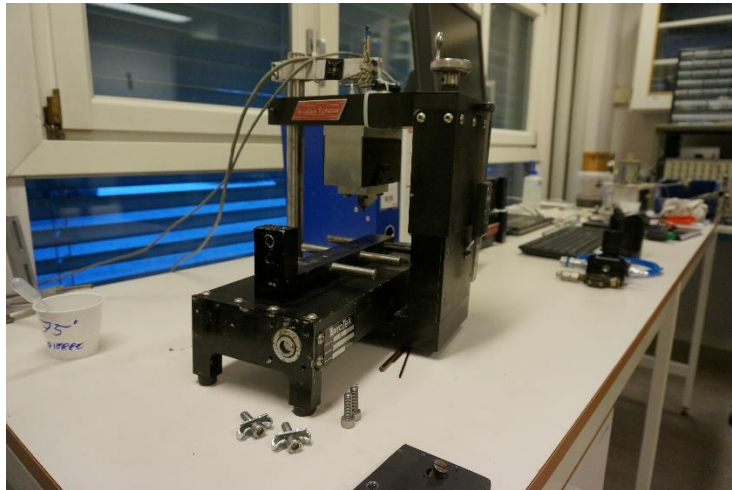


Figure 3.1: Original test rig.

3.2 Extra Features



Figure 3.2: Test rig vibration tool.

To test the effect of ultrasonic vibration, a device (Figure 3.2) was fabricated, to fit onto the original test rig. Technical drawings of the device can be found in Appendix A. The actuator used was a PPA60L (Appendix E) powered by LC75C and LA75C signal transformers delivered by Cedrat Technologies. The LabView program described in chapter 3.2.2 recorded the signal from the frequency generator. The frequency generator controls the output from the transformers.

3.2.1 Force Reduction by Vibration

To measure the effect of UAV on the force needed to cut the rock, the original test rig includes all the needed features. However, it is important to be aware that the modifications done to the rig by the vibration device, effects the results on the force readings. This implies that experiments performed without the modification is not comparable with tests performed with the modifications. Test performed with the cutter mounted for 20 μ m amplitude and for 32 μ m amplitude will show different force readings and should not be directly compared.

3.2.2 Stick-Slip Reduction by Vibration

In order to test the effect of UAV on stick slip behavior, the rig was designed with the possibility to move independently from the original test rig, and springs to store energy like a twisting drill string (Figure 3.3). The three springs located closest to the actuator, takes all the force from the cutting movement, the other three is there to keep it in place and soften the impact from severe slips. The spring configuration was decided by testing. Soft enough to give some movement, and stiff enough to keep it “floating”. During the stick-slip test, the

configuration was identical in the front and back row: one C04800721000M and two 13190. Detailed information about the springs can be found in Appendix D.



Figure 3.3: The rig showing sliding plate and springs.

To measure the stick-slip, a linear slider potentiometer was connected (Figure 3.4). The potentiometer measures how long the cutter blade is pushed back, relative to the measuring unit. The potentiometer is connected to a circuit board (Appendix B) to process the signal into being compatible with NI USB-6009. Through the NI USB-6009, the data is loaded into LabView.

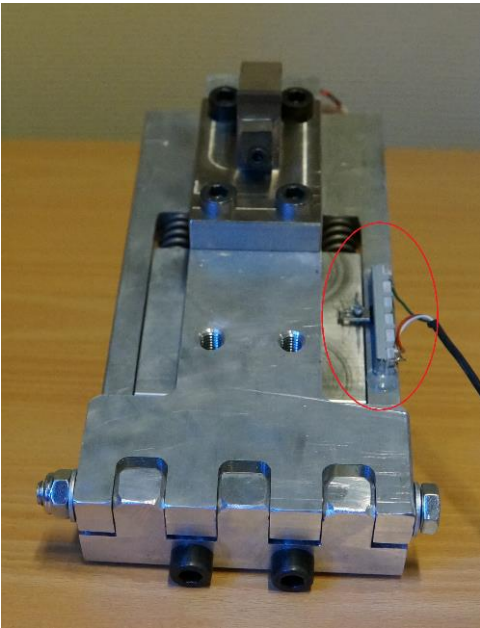


Figure 3.4: Potentiometer for stick slip measurement.

A LabView program was made to record the frequency and stick-slip displacement. The program code can be found in Appendix F. Figure 3.5 shows the LabView program. LabView plots the stick-slip displacement and frequency in two different windows, with the opportunity to export the data to Excel.

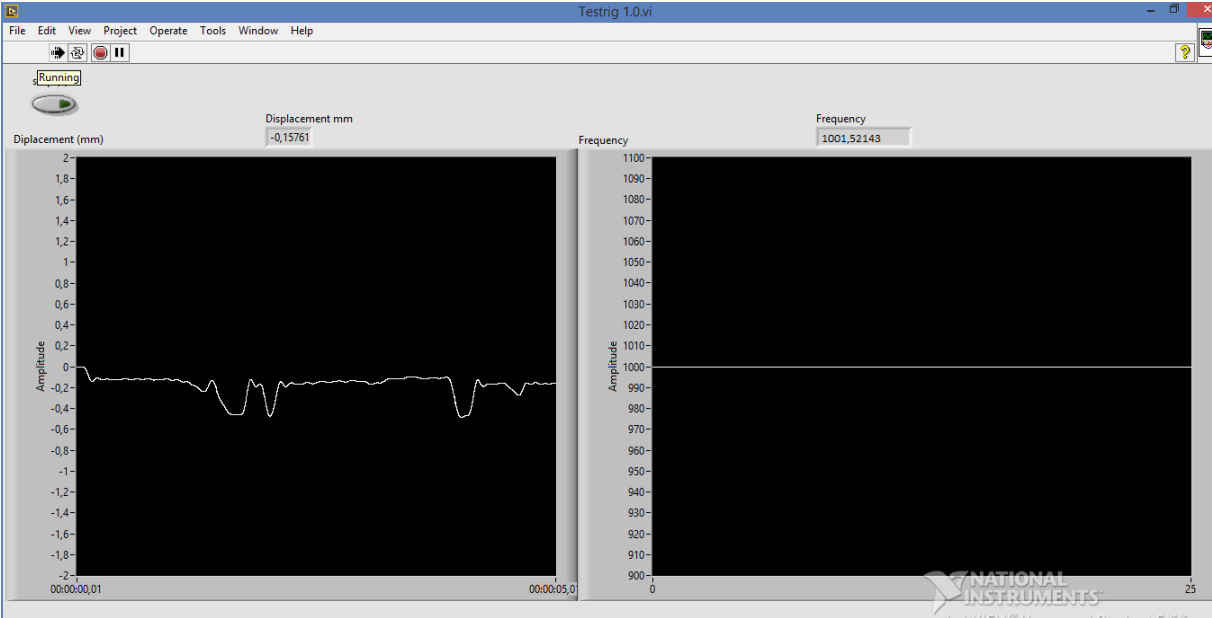


Figure 3.5: LabView program, displacement to the left, frequency to the right.

To lock the stick slip mechanism for the other tests, four lock blocks were introduced, as illustrated in Figure 3.6.

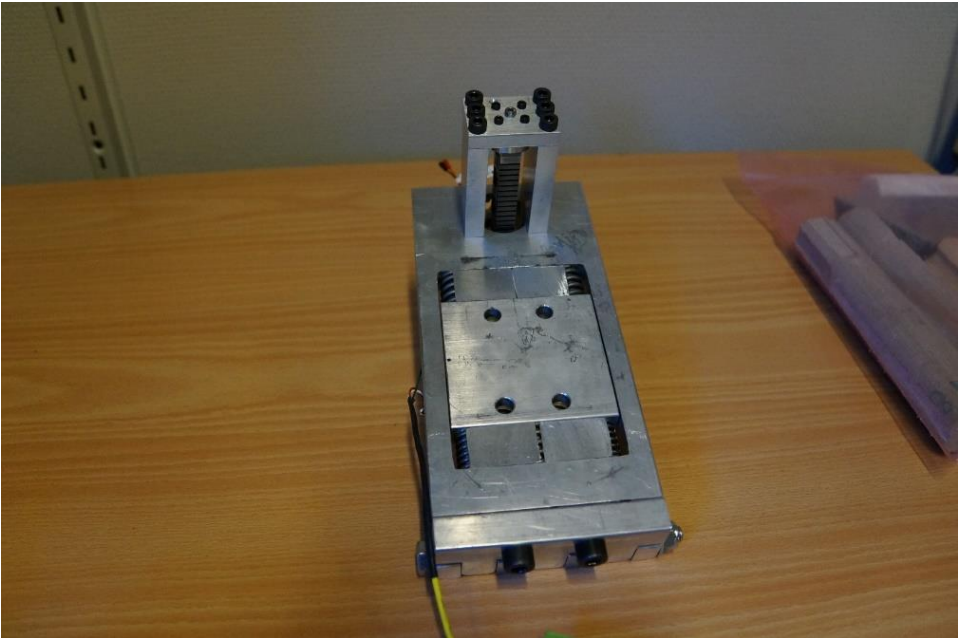


Figure 3.6: Lock tool, four blocks between the springs.

3.2.3 Vibration Effect on Wear

The original PDC blade were changed out with steel blades. Four numbered copies of the PDC blade were made as shown in Figure 3.7. The PDC blade is not suitable for this test due to the limited time and amount of scratching needed to show any signs of wear on a PDC blade.

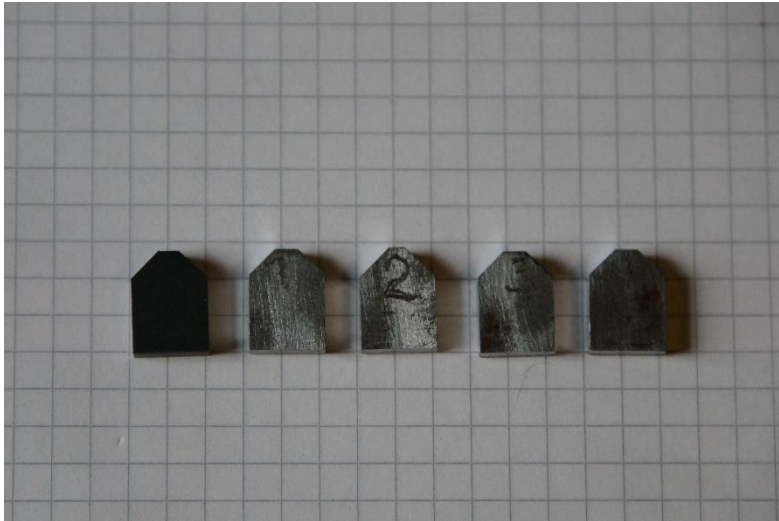


Figure 3.7: PDC blade to the left and four steel copies to the right.

To be able to present a valid comparison of the wear on different blades, microscopy analysis was needed. An Alicona Conofocal Infinite Focus Microscope (IFM) was used for documentation. More information about the Alcona IFM can be found at (Alcona.com 2015). The identification was conducted according to the following procedure on each blade:

1. Wash the blade with Acetone to remove small particles and grease.
2. Blow dry the blade to dry of the Acetone.
3. Start documentation in the IFM as soon as possible after cleaning.
4. Run scratch test.
5. Repeat point 1-3.
6. Compare the wear on each blade.

3.3 Experimental Setup

The experimental setup carried out in this project, listed as a procedure:

1. Install the high frequency vibration device, with the wanted springs or lock tools.
2. Clamp the selected rock sample to the test rig (Figure 3.8). Make sure that rig components do not crash into each other (metal to metal) during a scratch test.
3. Calibrate the measuring equipment (set to zero). Set vertical and horizontal zero point.
4. Adjust to wanted cutting depth and set wanted cutting length and speed.
5. Set wanted frequency if any, to the actuator. Can also be adjusted during the test.
6. Press start. If recordings of frequency and displacement is to be taken, press start on the LabView program at the same time.

N.B. The first 1-3 scratch runs over a sample are normally poor. It takes at least one run before the surface is even and the whole width of the blade touches the rock sample.

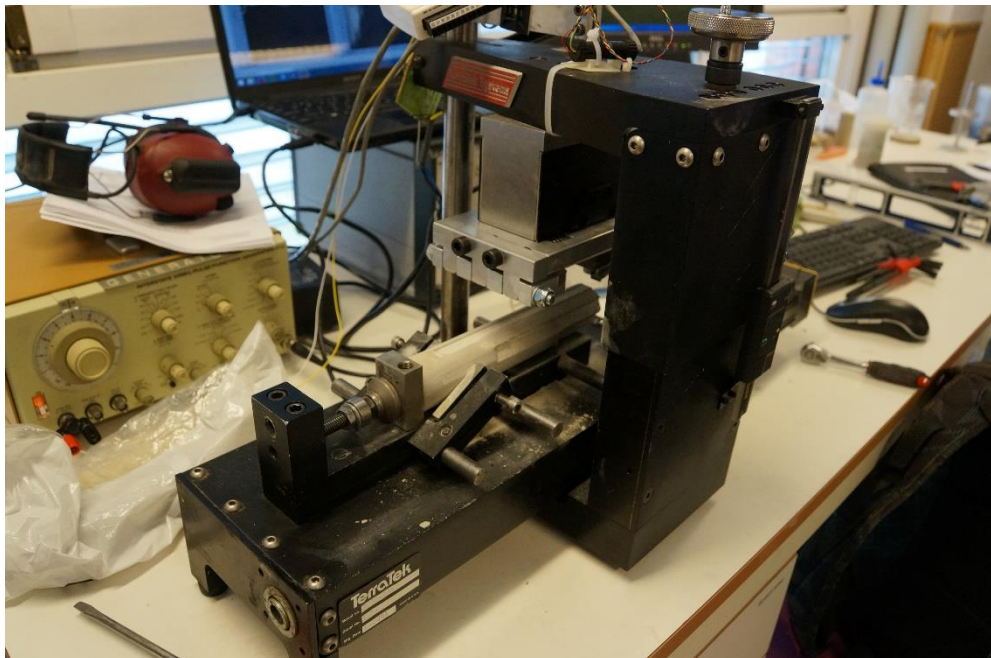


Figure 3.8: Securing the rock sample.

4 Results

This chapter presents, the results obtained from the experimental work and a technical design sketch for integrating ultrasonic vibration into a well tractor assembly.

4.1 Experimental Results

The results from the experimental work are presented in the next subsections. In total, over 70 scratch tests were performed, the results presented were picked out to represent the overall impression. All tests were performed on either Berea sandstone, Grunnes soapstone or Dionysos marble (Figure 4.1). Marble is significantly harder than the other two samples.



Figure 4.1: Stones used for testing, from the left: Berea Sandstone, Grunnes Soapstone and Dionysos Marble.

All tests are performed with a cutting blade of 10mm. The amplitude for all tests except for the 20 μ m amplitude test was run with 32 μ m vibration.

4.1.1 Force Reduction by Vibration

In the setup for force reduction by vibration, the effect of ultrasonic vibration with respect to force is presented. Figure 4.2 illustrates that presence of vibration generally is better than no vibration, but some frequencies are better than others. From Figure 4.2 it is possible to see a significant decrease in force around 500Hz, 1000Hz and 1200Hz. These frequencies were used in the next tests, where each of these frequencies were studied more thoroughly. 500Hz was skipped for the tests on soapstone and marble because 1000- and 1200Hz gave much better results.

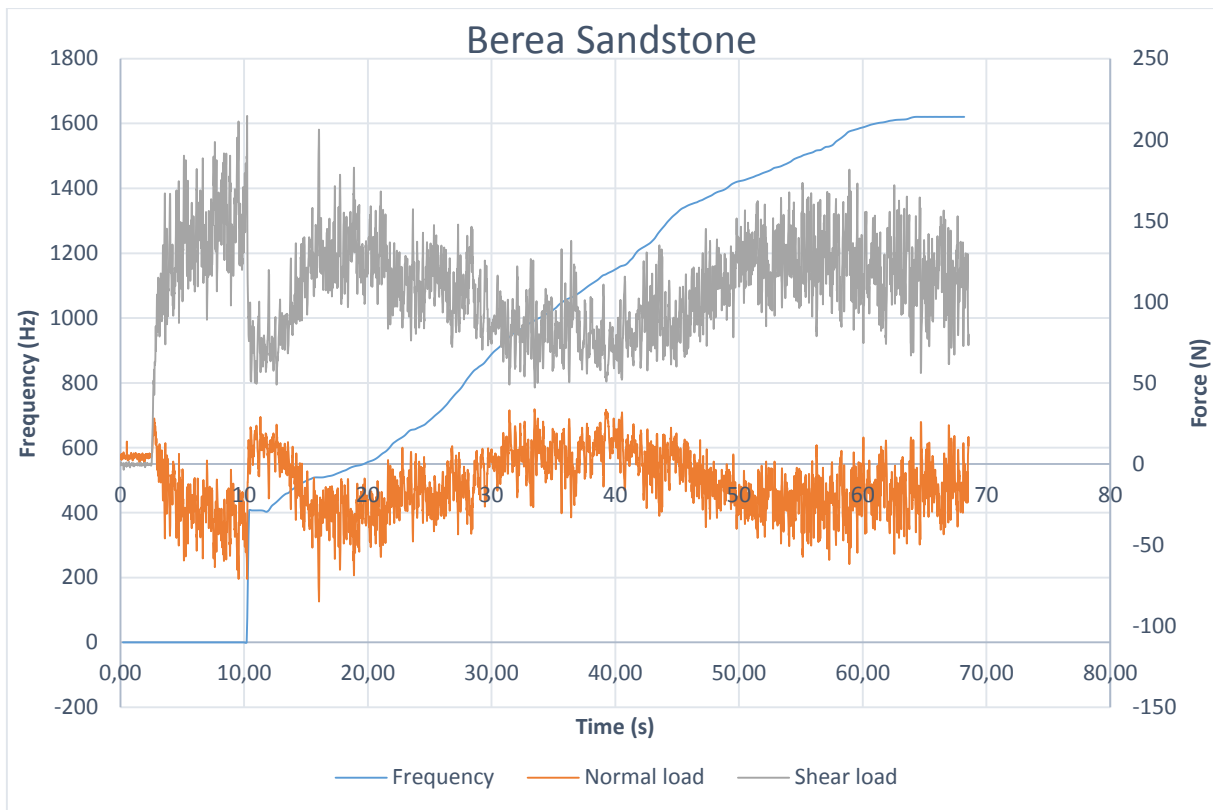


Figure 4.2: Scratch test with increasing frequency vibration.

From the diagrams (Figure 4.3, Figure 4.5 and Figure 4.7) it was possible to control that the different test runs followed the same pattern, signaled by low variation between the runs. For example, a sudden change in the rock sample on one of the tests would show a sudden peak in only one of the curves.

The column charts (Figure 4.4, Figure 4.6 and Figure 4.8) show the average force values for each run. These values were the best for directly comparing of the effect of each frequency. From the figures, we see that 1000- and 1200Hz were similar. 1000Hz gave slightly better result; therefore, 1000Hz was used for the speed and frequency test, and in the wear and stick-slip analysis.

Force tests were performed at 0,5mm cutting depth for the sandstone and soapstone and 0,3mm for the marble.

Berea Sandstone

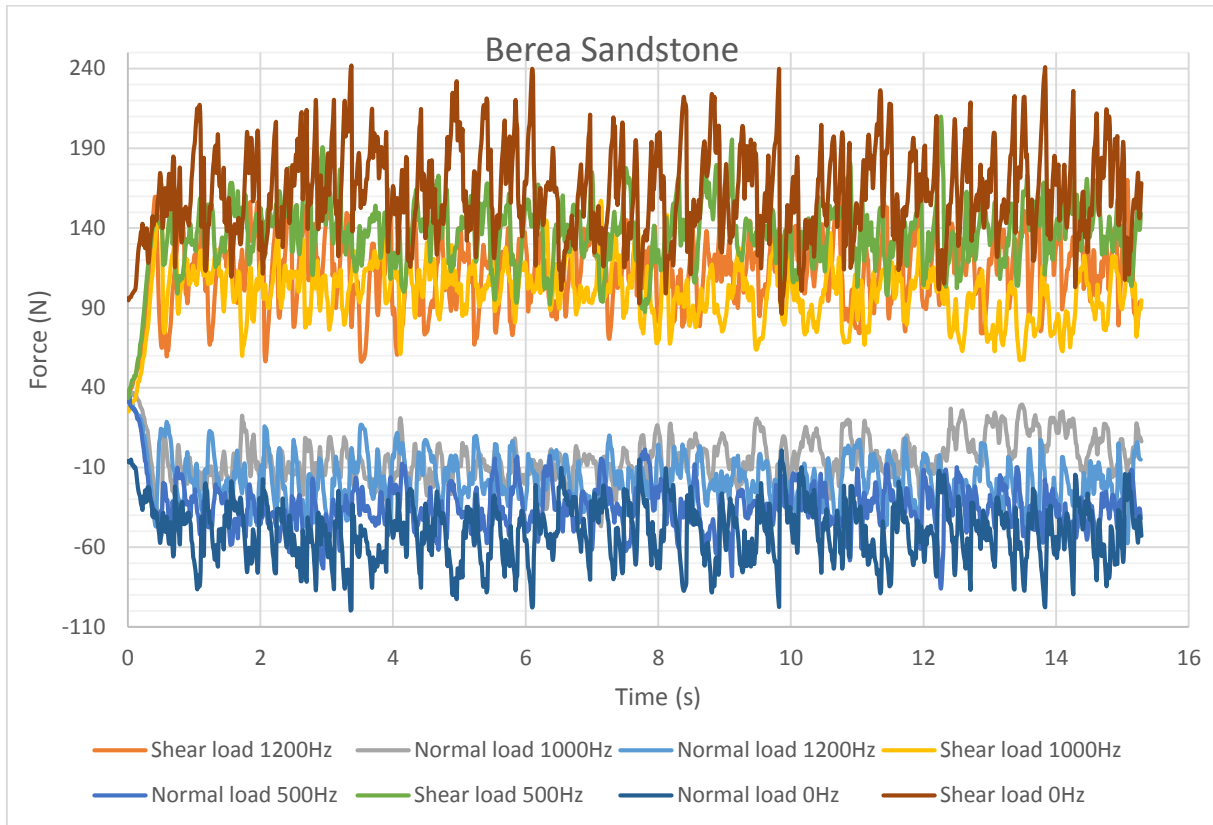


Figure 4.3: Berea sandstone, scratch diagram.

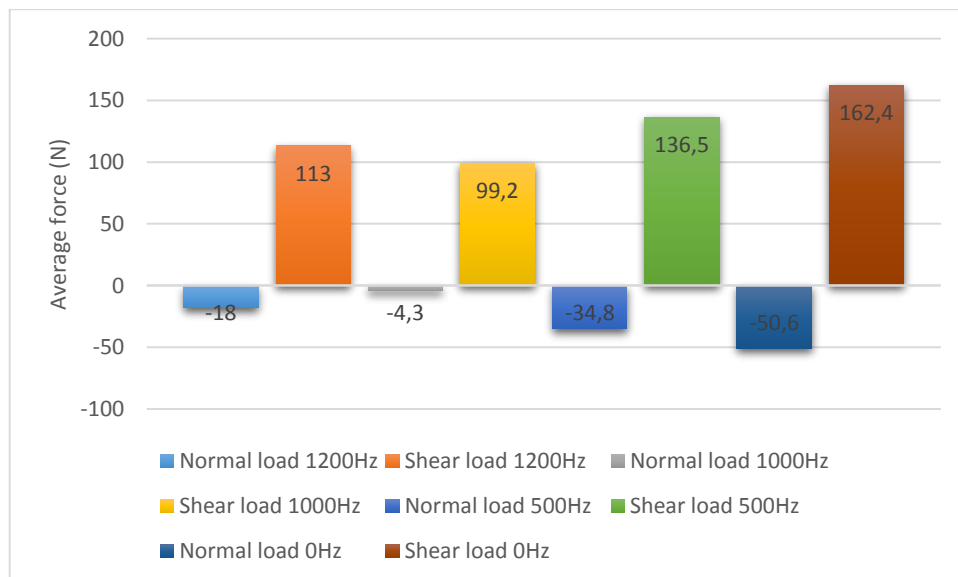


Figure 4.4: Berea sandstone, average scratch values.

Grunnes Soapstone

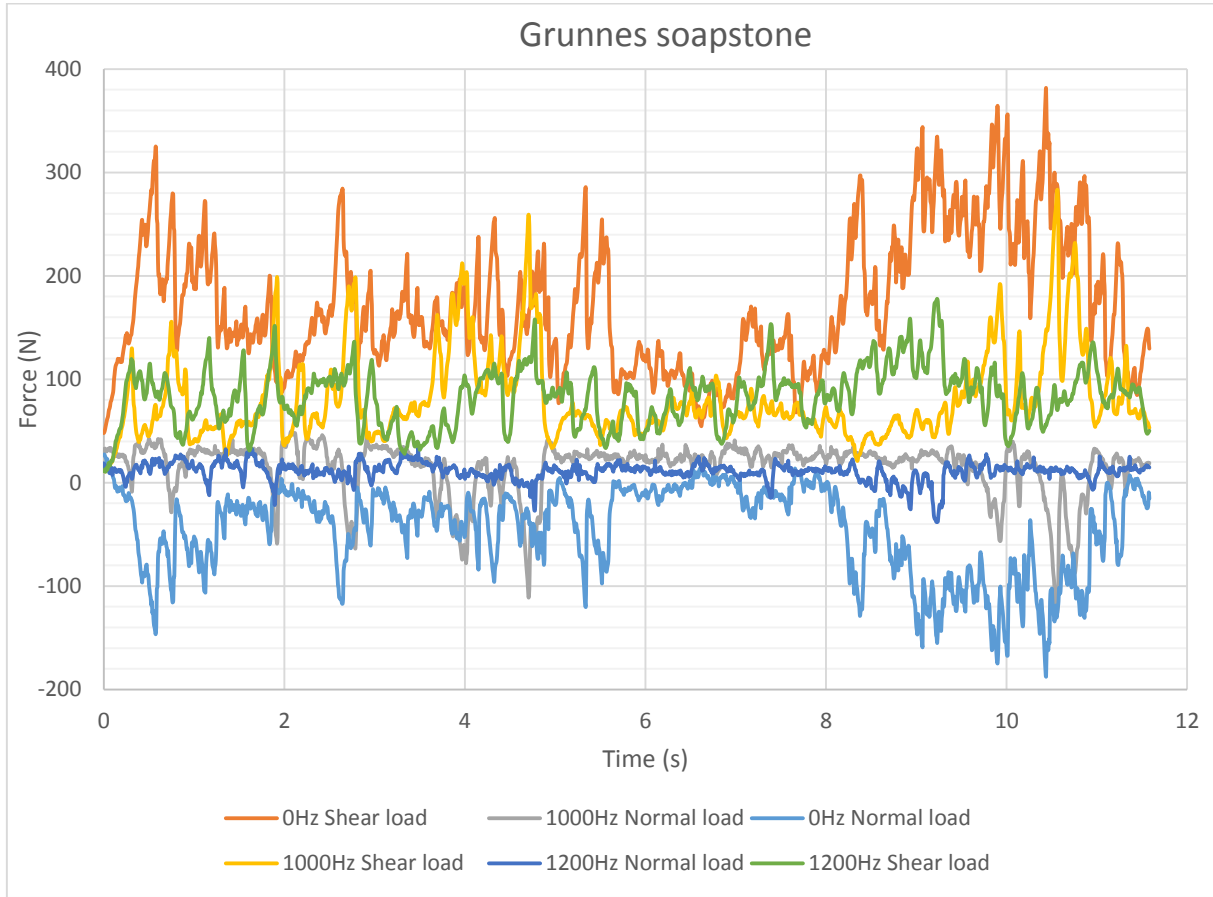


Figure 4.5: Grunnes soapstone, scratch diagram.

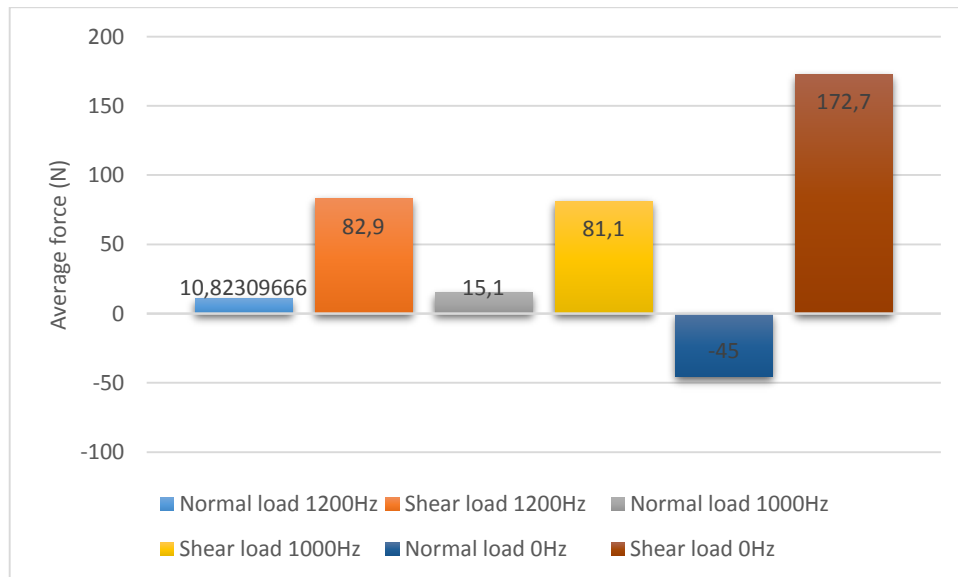


Figure 4.6: Grunnes soapstone, average scratch values.

Dionysos Marble

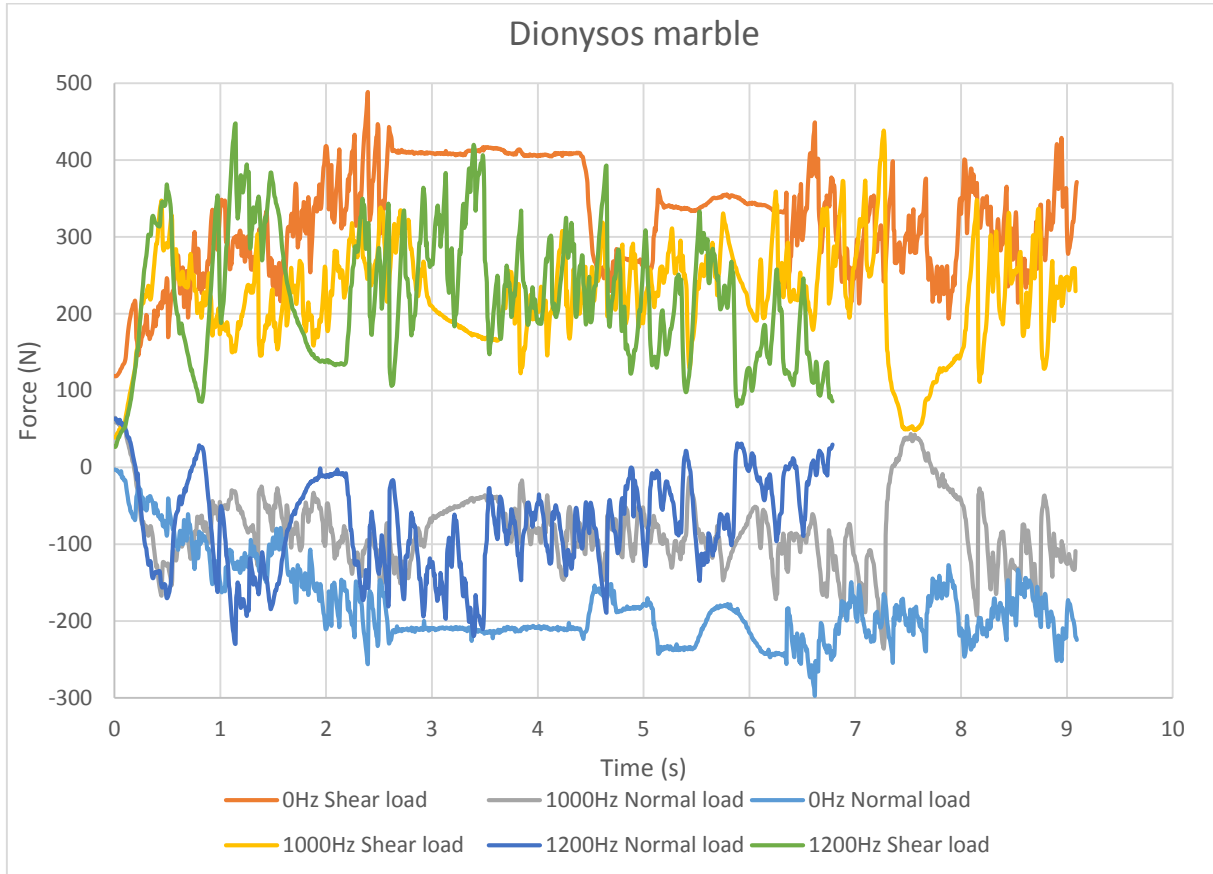


Figure 4.7: Dionysos marble, scratch diagram.

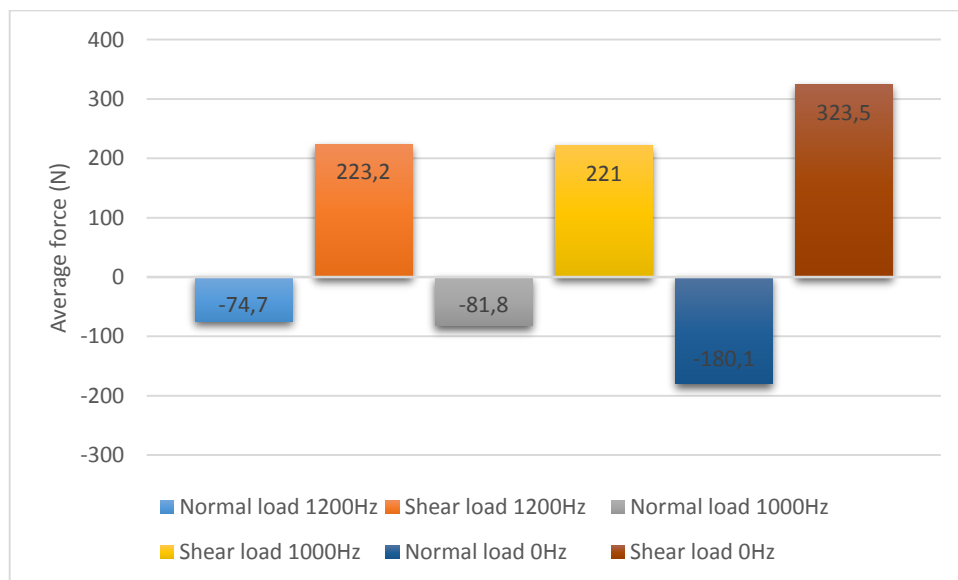


Figure 4.8: Dionysos marble, average scratch values.

Speed and Amplitude

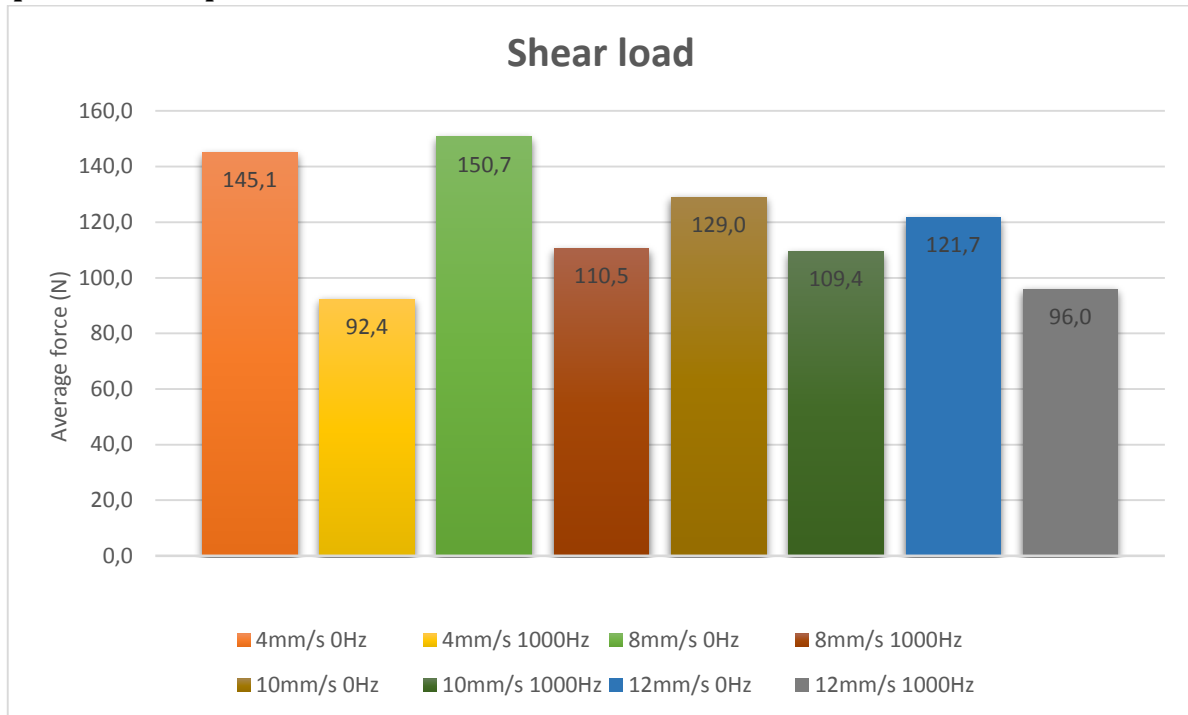


Figure 4.9: Average scratch values for certain speeds.

Figure 4.9 indicates that the effect of ultrasonic vibration decreases with increasing cutting speed, but at 12mm/s the test shows signs of improvement again. The tests were performed with 0.3mm cut depth on Berea sandstone.

For the amplitude test there was no graphical illustration because the 20- and 32 μ m displacement cannot be directly compared (section 3.2.1). Instead a comparison in percentage force reduction is given. The tests are performed with 0.5mm cut depth and 4mm/s cutting velocity in Berea sandstone.

20 μ m displacement:

0Hz – 296,7N shear load

1000Hz – 259,0N shear load

$$\text{Force Reduction by Vibration} = \frac{(296,7 - 259)}{296,7} \times 100 = 12,7\%$$

32 μ m displacement:

0Hz – 162,4N shear load

1000Hz – 99,2N shear load

$$\text{Force Reduction by Vibration} = \frac{(162,4 - 99,2)}{162,4} \times 100 = 38,9\%$$

According to these tests, the vibration amplitude has a major impact on the efficiency of the ultrasonic vibration.

4.1.2 Stick-Slip Reduction by Vibration

The performed tests failed to reproduce any real stick-slips. The largest difference in the stick-slip effect with respect to vibration was that tests performed with vibration slipped more frequently, see Figure 4.10. The displacement shows some variation from test to test; in general, the displacement was slightly smaller for tests run with vibration than without. The stick-slip tests were conducted in Berea sandstone.

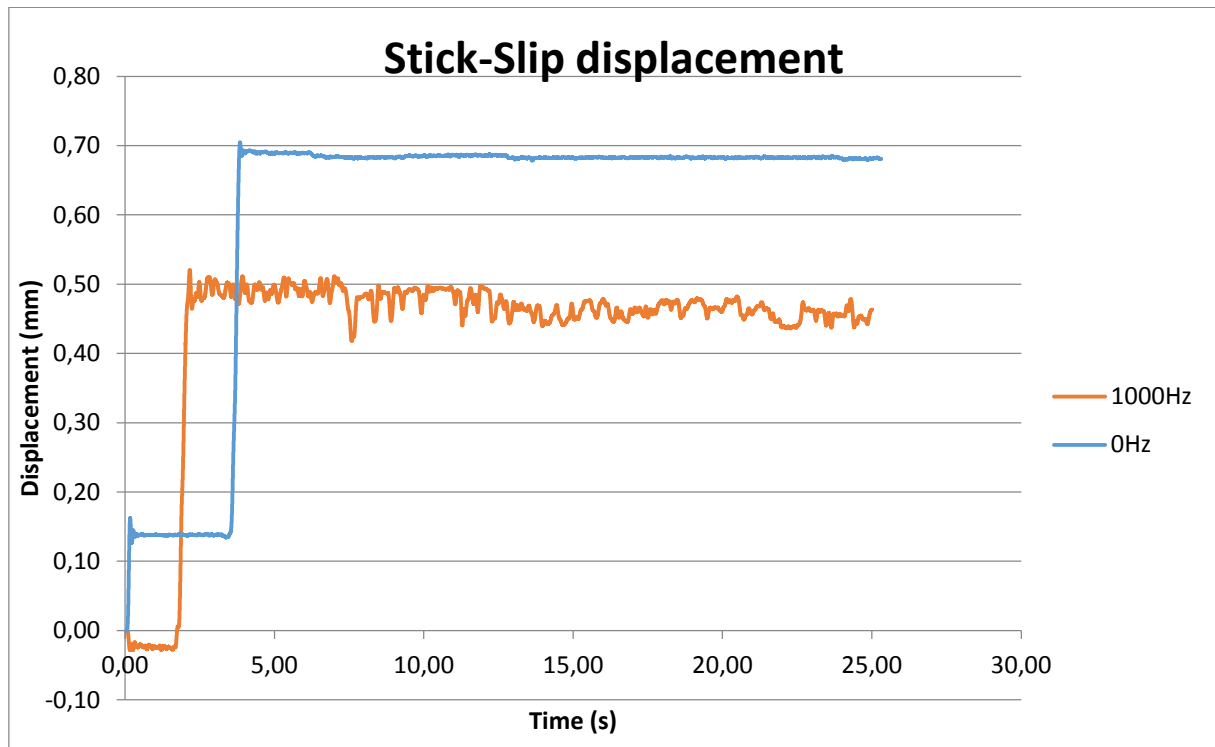


Figure 4.10: Stick-Slip curve.

4.1.3 Vibration Effect on Wear

The documentation carried out using the IFM microscope resulted in 2D and 3D pictures of each cutter blade, before and after scraping.

Figure 4.11 shows the initial 2D pictures of the blades. The similarity between the blades are so high that comparison in 3D is based on the blades looking the same before scratch tests. All pictures are taken in the same corner of the cutter blades, the corner of interest is the one up to the right for the 2D pictures. The pictures in 3D are from the front of the blade with the corner of the cutting blade down to the left. 2D pictures are magnified 2,5 times and 3D pictures are magnified 20 times.



Figure 4.11: 2D X2,5 initial picture of blade 1 to 4.

This experiment was conducted on two different stone types. Berea sandstone and Dionysos marble.

For comparison the initial and final 2D pictures were placed on top of each other, the green pattern shows the initial blade. The 0Hz blade is also mirrored for direct comparison.

From Figure 4.12 and Figure 4.15 it is clear that the cutter blades subjected to ultrasonic vibration show a higher degree of wear. The wear on the cutter were higher for tests performed using marble compared to sandstone. However, in both cases the non-vibration cutter blades shows more wear on the edges compared with the ones exposed to vibration. The green areas in Figure 4.12 and Figure 4.15 are measured by using ImageJ (program for measurements on pictures), the overall wear difference are as follows:

Berea sanstone:

$$0\text{Hz wear} = 1,231\text{mm}^2$$

$$1000\text{Hz wear} = 1,324\text{mm}^2$$

$$\text{Increased wear} = \frac{(1,324 - 1,231)}{1,231} \times 100 = 7,5\%$$

Dionysos marble:

$$0\text{Hz wear} = 0,854\text{mm}^2$$

$$1000\text{Hz wear} = 1,029\text{mm}^2$$

$$\text{Increased wear} = \frac{(1,029 - 0,854)}{0,854} \times 100 = 20,5\%$$

The wear on Berea sandstone was larger because the rock sample for the Berea sandstone was much longer than the marble, and the test used the whole length of the rock sample.

An interesting detail seen on the 3D pictures (Figure 4.13, Figure 4.14, Figure 4.16 and Figure 4.17) is that the blades with vibration build up a ridge on the tip of the blade. This ridge could affect the wear in long term. If the test had lasted for a longer time, the amount of wear on the non-vibration blades and the vibration blades could have equalized. Larger 3D pictures with profile indication can be found in Appendix G.

Berea Sandstone

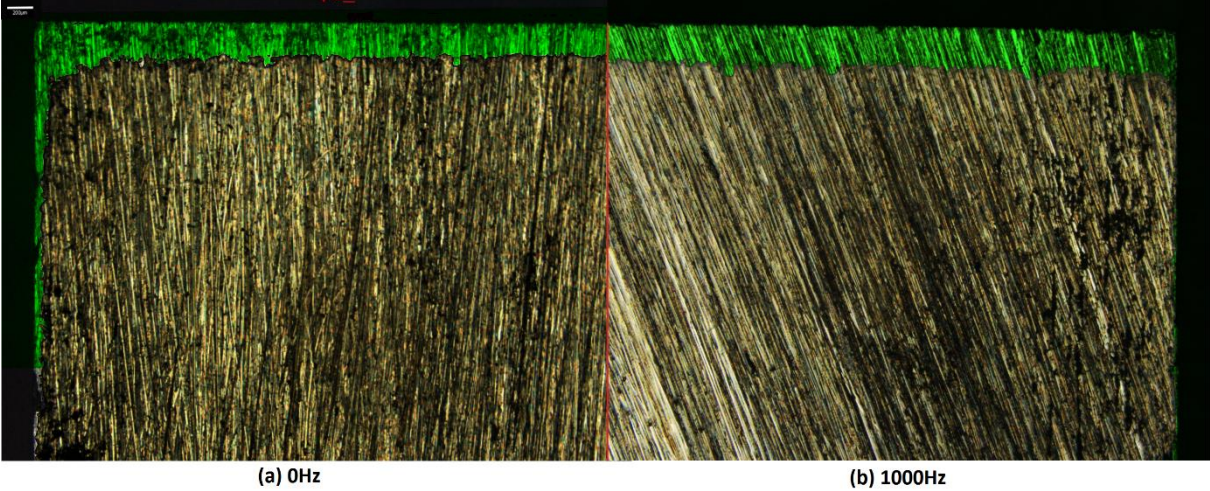


Figure 4.12: 2D X2,5 comparison of cutter blades after test on Berea sandstone, green section shows the wear. The small white stripe in the upper left corner is a measurement scale, 200µm.

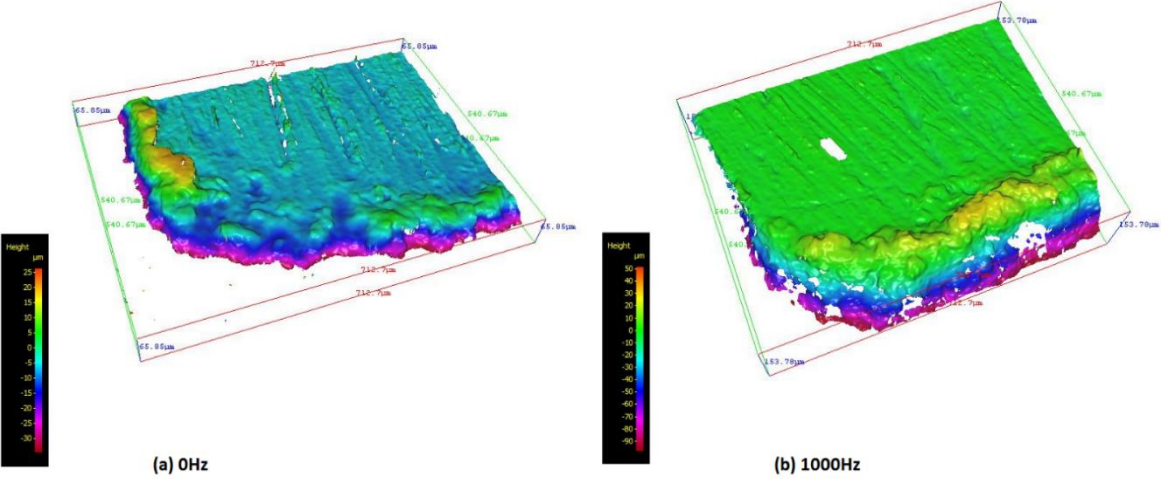


Figure 4.13: 3D X20 comparison from the front of cutter blade after test on Berea Sandstone, picture with profile indication.

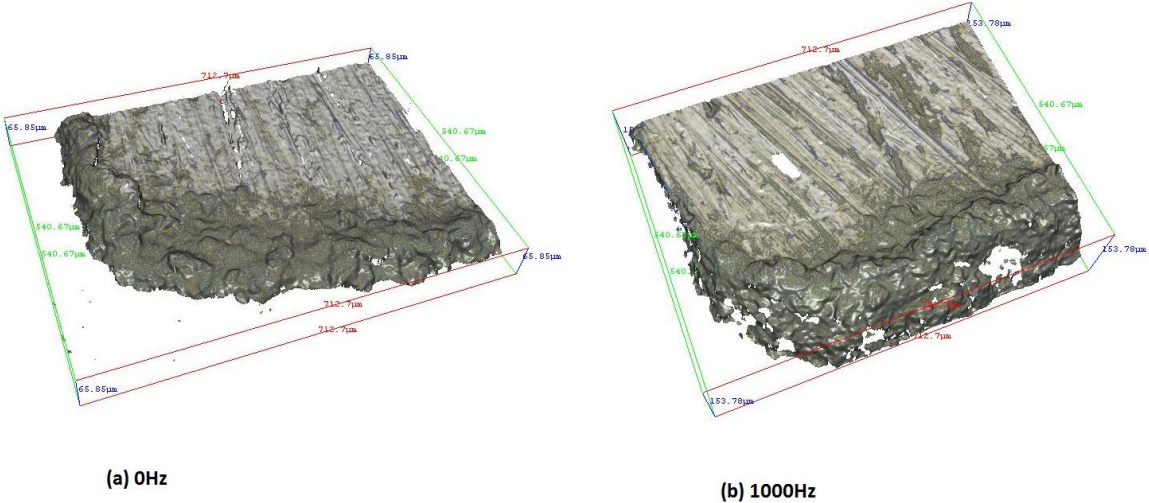


Figure 4.14: 3D X20 comparison from the front of cutter blade after test on Berea Sandstone.

Dionysos Marble

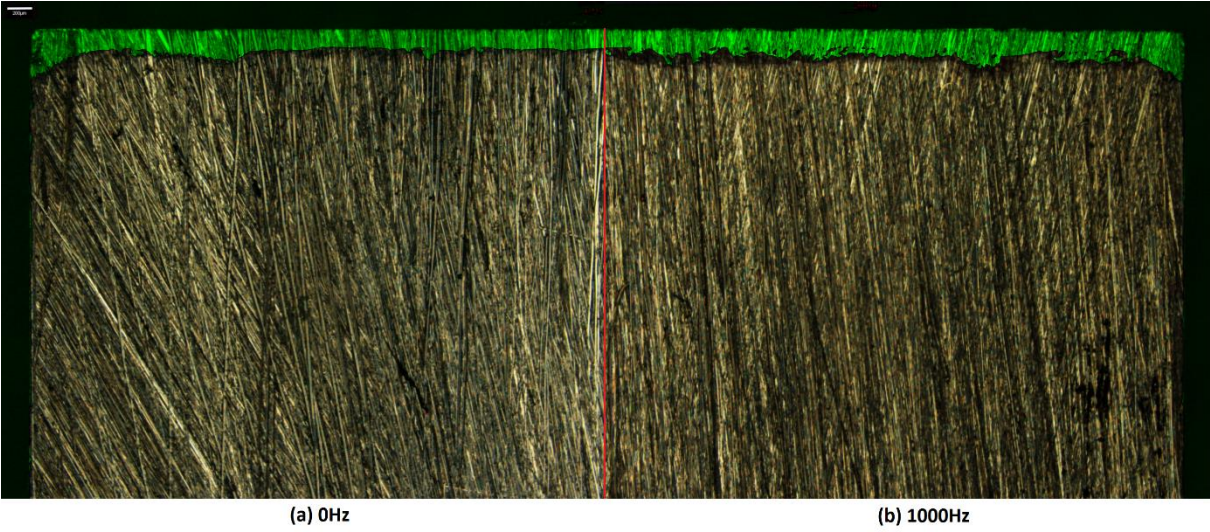


Figure 4.15: 2D X2,5 comparison of cutter blades after test on Dionysos Marble, green section shows the wear. The small white stripe in the upper left corner is a measurement scale, 200µm.

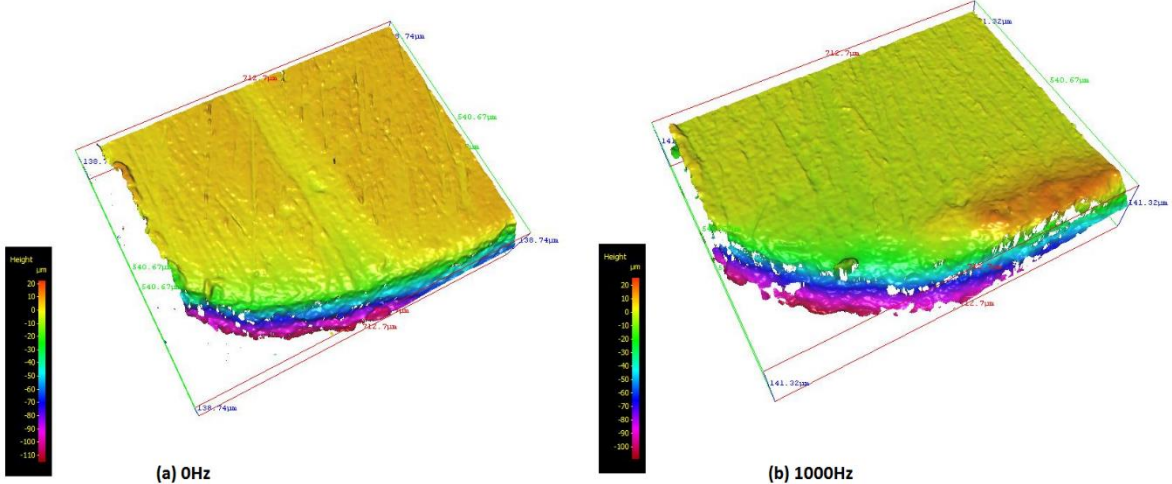


Figure 4.16: 3D X20 comparison from the front of cutter blade after test on Dionysos Marble, picture with profile indication.

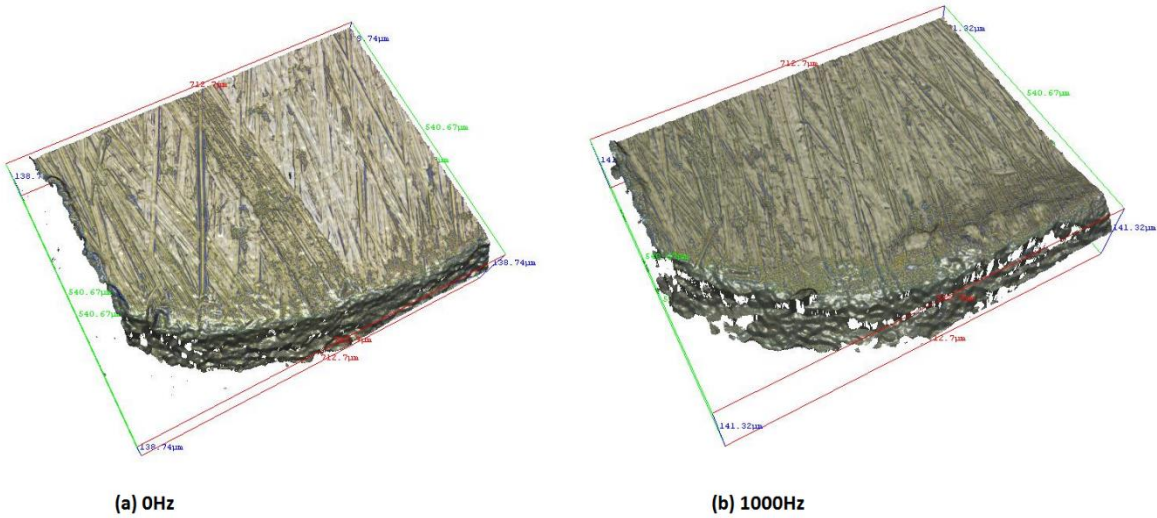


Figure 4.17: 3D X20 comparison from the front of cutter blade after test on Dionysos Marble.

4.2 Ultrasonic Assisted Tractor Operation

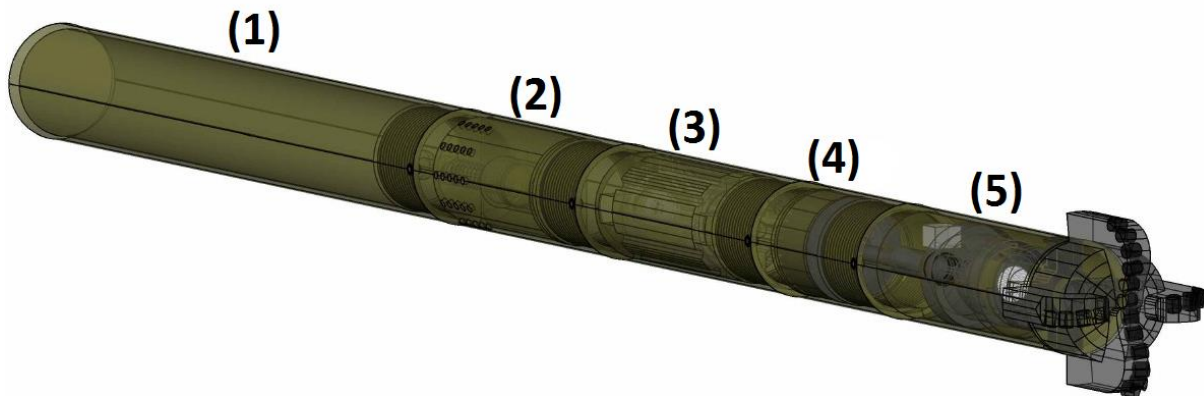


Figure 4.18: X-ray picture of ultrasonic tractor equipment, divided in five sections.

In this sub-chapter, a proposed solution for integrating ultrasonic vibration into well tractor equipment is presented. The equipment is divided into five sections plus the drill bit. Each section has a special function, and are screwed together to form the Ultrasonic Assisted Tractor. This design is used to simplify repairs, and make it possible to optimize the equipment for each operation. Connection to the tractor is omitted, because it needs to fit the connection from the desired manufacturer.

It has only been made calculations for the piezoelectric actuator. The rest is a principal sketch. The drawing is made in a scale giving the body diameter of 80 mm and the drill bit diameter of 120 mm.

Figure 4.18 shows the different sections of the system:

1. Electrical
2. Pressure equalization
3. Motor
4. Gear
5. Actuator

The next sub chapters present the different sections. The pictures shown will be in x-ray vision to see the details better. The natural metallic color is used if nothing else is stated. The main body of the equipment is made of titanium for corrosion and wear resistance.

4.2.1 Electrical

The electrical equipment is not shown in details. Wires to the motor and the actuator are not shown in the figures, but there is sufficient space. The electrical section will consist of the following units:

- Voltage transformer, for the actuator and possibly the motor.
- Sine inverter/controller for the actuator.

There are some strict requirements for these components:

- Pressure resistant, more than 1000bar.
- Fit inside a tube with inner diameter of 74mm.
- Keep energy loss at a minimum.

The voltage transformer is one of the components appropriate to replace for optimization in each well intervention, depending on cable length.

4.2.2 Pressure Equalization

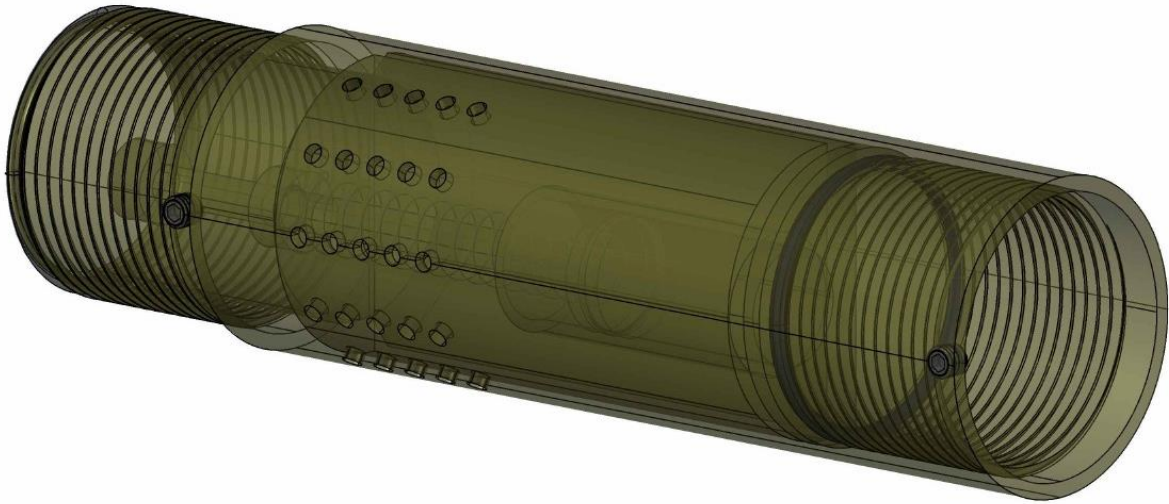


Figure 4.19: Pressure compensation section.

To withstand the extreme pressures in oil and gas wells, the equipment is designed to be filled with silicon oil and pressure compensated. Silicone oil is an electric insulator, so it do not damage the electric components. Figure 4.19 shows the holes letting the fluid or gas from the well into the compensation cylinder (Figure 4.20). The spring in the system is used to ensure one bar overpressure.

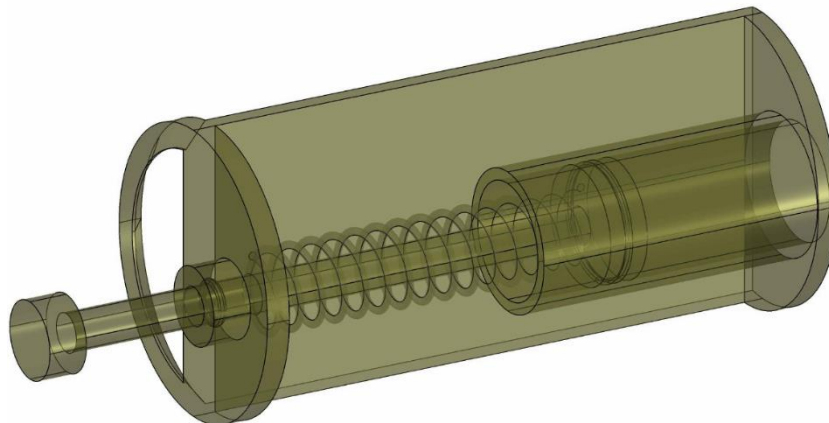


Figure 4.20: Pressure compensating cylinder.

The main reasons for using pressure equalization instead of building it strong enough to withstand the pressure are:

- Thinner walls to give more space for components.
- Pressure resistant seal on the shaft to the drill bit would create a lot of friction when you got a spinning shaft that also moves in and out.

4.2.3 Motor

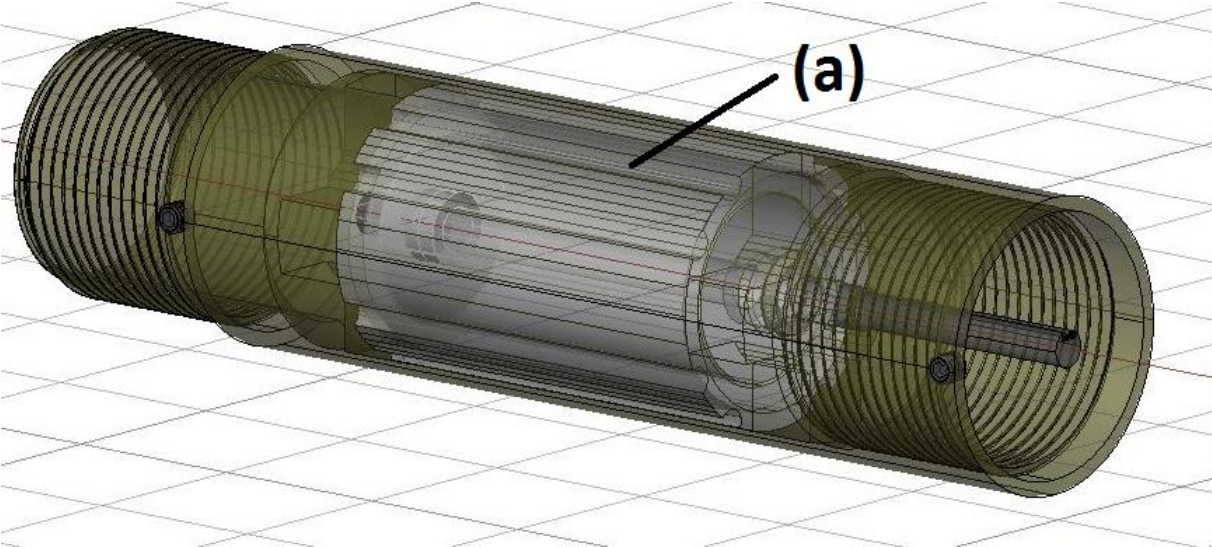


Figure 4.21: Motor section, (a) electric motor.

The brighter part (a) in Figure 4.21 illustrates an open electric motor, dedicated for operation in liquid fluids. The electric motor is also relevant to change depending on well depth to achieve optimum speed for the operation. It is preferable to avoid using voltage transformer to reduce loss in the electrical system.

4.2.4 Gear

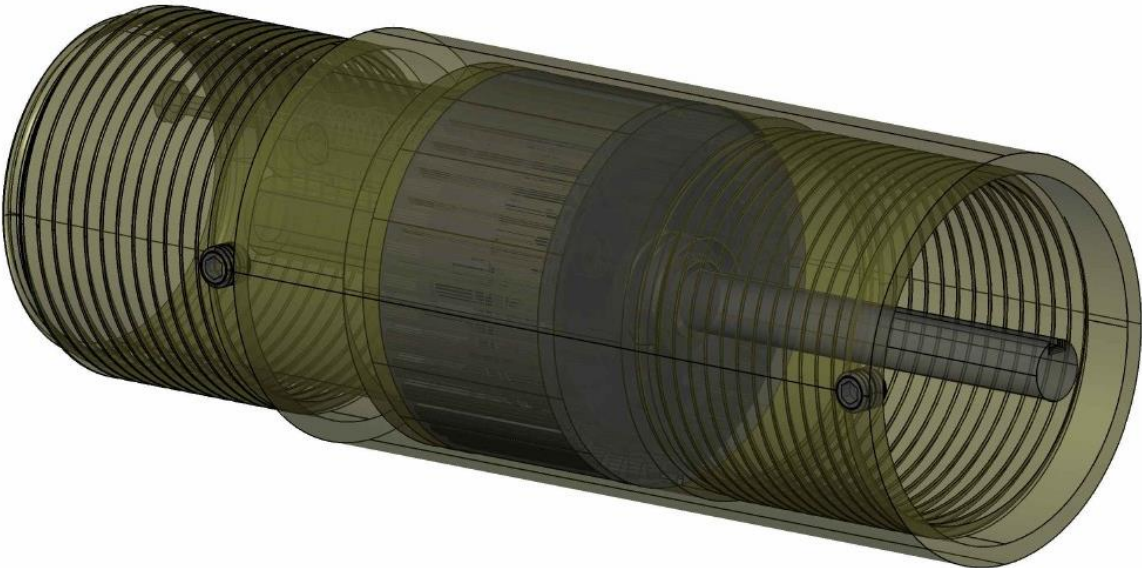


Figure 4.22: Gear section.

Gear is needed to keep the motor running at an optimum speed for energy saving, and to achieve a high torque on the drill bit.

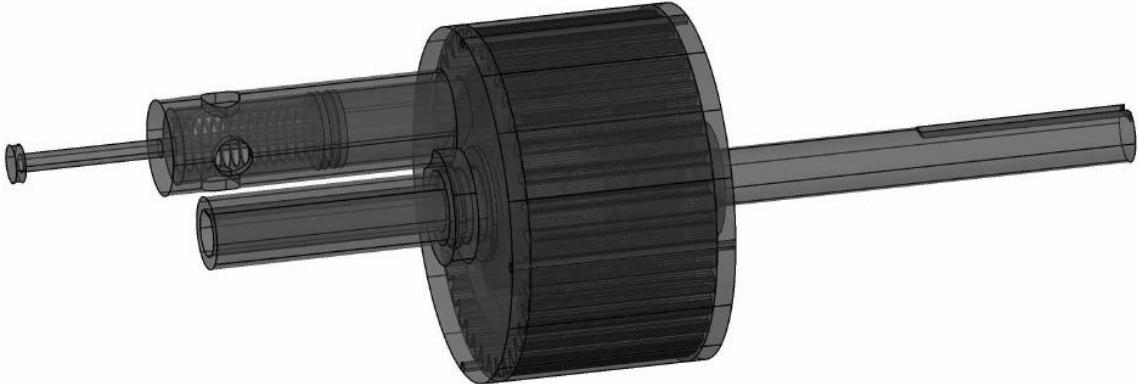


Figure 4.23: Gear box with pressure equalizer.

The gearbox is designed with an own pressure equalizer. To ensure smooth running and long lifetime, the gears should run in gear oil. Keeping the gear oil separated also prevents potential metal chips from the gear to short-circuit any electrical components.

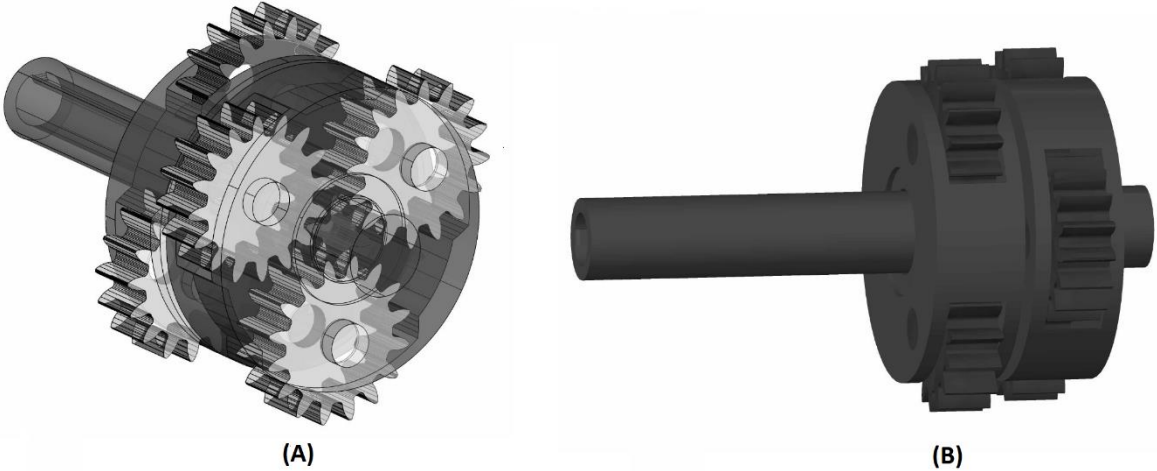


Figure 4.24: Gear wheels, (A) x-ray- and (B) realistic-view.

A planetary gear is used. Planetary gears are compact and has outstanding power transmission efficiency (Lu and Jin 2011). The gear has a ratio of 14:1, giving 150rpm at drill bit when the motor holds 2100rpm.

4.2.5 Actuator

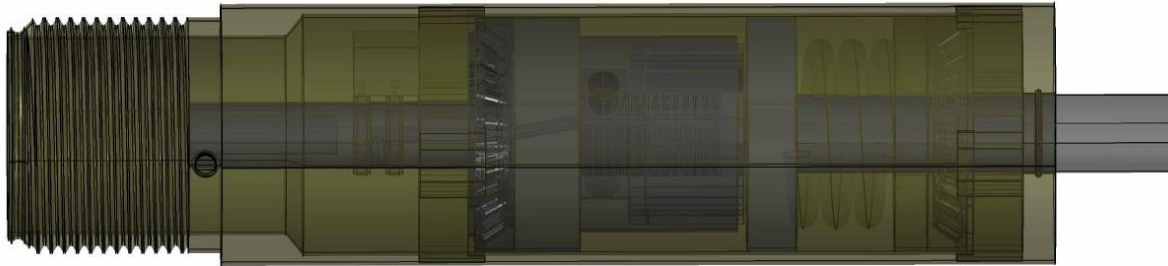


Figure 4.25: Actuator section.

The main focus in the design proposal is directed to the actuator section. Figure 4.26 shows the components inside the actuator section. Presented in colors for easier identification.

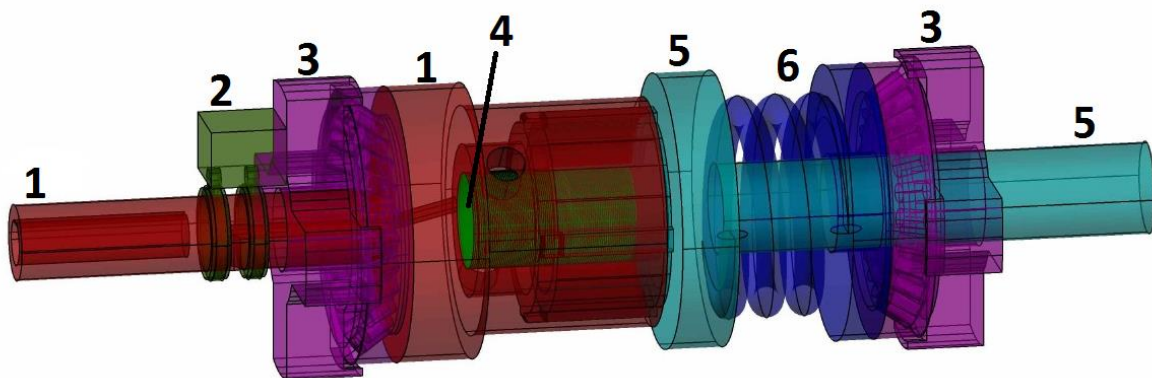


Figure 4.26: Inside the actuator section, in colors.

1. (Red) Shaft from the gearbox and lower actuator holder. Inside you can see the path for the wires to the actuator.
2. (Dark green) Electric transfer for the actuator through the shaft.
3. (Pink) Foundation for the actuator system and tapered roller bearings.
4. (Green) Piezoelectric actuator.
5. (Turquoise) Upper actuator holder and drill bit shaft.
6. (Blue) Spring and spring foundation.

Upper and lower actuator holder is designed with grooves to fit into each other, transferring the rotational movement and allowing axial movement.

The spring is used to ensure that the drill bit vibrates, pushing the upper actuator holder and shaft towards the actuator, and keeping the lower actuator holder against its foundation.

Tapered roller bearings are used because they can withstand both axial and radial forces.

Piezoelectric actuator

The design process is based on the equations presented in section 2.3.1. The following actuator specifications and operating requirements are used to design the actuator.

Displacement:

50 μ m gives some room for reduction in displacement caused by external forces. The actuator does not need to run at max voltage to achieve 32 μ m displacement. Alternatively the displacement can be increased.

50 μ m gives an actuator length of 50mm, using the regular electric field to minimize the amount of electric controllers needed.

Force:

Assuming scale deposition in the production tubing is similar to sandstone with respect to drilling. Maximum compressive strength of sandstone: 140N/mm² (Mineralszone 2015).

An approximation was made for the contact area between the teeth in the drill bit and the formation being drilled. By putting all the teeth in a continuous line from the center of the drill bit and out to the edge a line of 60mm is formed. The teeth are tilted slightly backwards giving a larger contact area than just the edge, approximately 60mm·2mm=120mm².

$$F=140\text{N}/\text{mm}^2 \cdot 120\text{mm}^2=16800\text{N}$$

External forces:

A spring will push the drill bit back against the actuator. The drill bit is not directly connected to the actuator in order to minimize the tensile loads acting on the actuator. The spring pushes back the drill bit after every push from the actuator.

$$k_{\text{spring}} = 78,5\text{N}/50\mu\text{m}=1570000\text{N}/\text{m}$$

The volume of the drill bit and the shaft is 0,51dm³. Using tungsten carbide for both the shaft and drill bit gives a total mass of 8kg. Tungsten carbide are used in the shaft because it is approximately two times stiffer than steel, thereby displacing the vibration better.

$$F_{\text{Drill bit}} = 8\text{kg} \cdot 9,81\text{m}/\text{s}^2=78,5\text{N}$$

In addition, 1000N push force from tractor.

For the actuator, PZT-4 (Morgan 2010) data is used for further calculations. PZT-4 and the specifications described above gives the following properties:

Youngs modulus E	$6,3 \cdot 10^{10} \text{Pa}$
Cross section A	$3,5 \cdot 10^{-4} \text{m}^2$
Length l	$0,05 \text{m}$
Max. nominal displacement	$5 \cdot 10^{-5} \text{m}$
Weight of shaft and drill bit	$8,0 \text{kg}$
k_{SPRING}	$392,4 \cdot 10^5 \text{N/m}$
Density PZT ρ_{PZT}	7500kg/m^3
U_{max}	150V
Frequency f	1000Hz
Layer thickness d_s	$1,0 \cdot 10^{-4} \text{m}$
Number of layers n	500
Dielectric constant in vacuum ϵ_0	$8,85 \cdot 10^{-12} \text{As/Vm}$
ϵ_{33}/ϵ_0	1300
ϵ_{33}	$1,15 \cdot 10^{-8}$

150V is the maximum voltage for multilayer piezo electrical elements, lowering the voltage reduces the displacement and the energy demand.

The cross section area was found by trial and error, until all requirements were fulfilled. The blocking force must be more than the crush force to have any effect if the drill hits scale of this roughness. More force also limits the displacement lost to the spring and drill bit. Too much extra force and the actuator will use an unnecessarily amount of energy. 350mm^2 was the final choice. The calculations are presented as follows.

Actuator stiffness:

$$k_{PZT} = \frac{E \cdot A}{l}$$

$$k_{PZT} = \frac{63 \text{GPa} \cdot 3,5 \cdot 10^{-4} \text{m}^2}{0,05 \text{m}}$$

$$k_{PZT} = 44,1 \cdot 10^7 \text{N/m}$$

Force generaion (block force):

$$F_{max} \approx k_{PZT} \cdot \Delta L_0$$

$$F_{max} \approx 44,1 \cdot 10^7 \text{N/m} \cdot 5 \cdot 10^{-5} \text{m}$$

$$F_{max} \approx 22050 \text{N}$$

Influence on displacement by external force:

By mass:

$$\Delta L_N \approx \frac{F}{k_{PZT}}$$
$$\Delta L_N \approx \frac{8,0kg \cdot 9,81m/s^2}{44,1 \cdot 10^7 N/m}$$
$$\Delta L_N \approx 2,5 \cdot 10^{-6}m$$

By spring:

$$\Delta L_R = \Delta L_0 \cdot \left(1 - \frac{k_{PZT}}{k_{PZT} + k_{spring}}\right)$$
$$\Delta L_R = 5 \cdot 10^{-5}m \cdot \left(1 - \frac{44,1 \cdot 10^7 N/m}{44,1 \cdot 10^7 N/m + 392,4 \cdot 10^5 N/m}\right)$$
$$\Delta L_R = 4,1 \cdot 10^{-6}m$$

To achieve 32 μ m displacement, the actuator needs to be adjusted to 38,6 μ m ($\Delta L_N + \Delta L_R + 32\mu$ m).

Resonant frequency:

To calculate the resonant frequency the effective mass must be calculated.

$$m_{eff} \approx \frac{m_{PZT}}{3} + m$$
$$m_{eff} \approx \frac{0,13kg}{3} + 8$$
$$m_{eff} \approx 8,044kg$$
$$f_0 = \frac{1}{2} \pi \cdot \sqrt{\frac{k_{PZT}}{m_{eff}}}$$
$$f_0 = \frac{1}{2} \pi \cdot \sqrt{\frac{44,1 \cdot 10^7 N/m}{8,044kg}}$$
$$f_0 = 11625Hz$$

Capacitance:

$$C = n \cdot \epsilon_{33} \cdot \frac{A}{d_s}$$

$$C = 500 \cdot 1,15 \cdot 10^7 \cdot \frac{A3,5 \cdot 10^{-4}m^2}{1,0 \cdot 10^{-4}m}$$

$$C = 2,0 \cdot 10^{-5}F$$

Average power:

$$P_a \approx C \cdot U_{max} \cdot U_{p-p} \cdot f$$

$$P_a \approx 2,0 \cdot 10^{-5}F \cdot 150V \cdot 150V \cdot 1000Hz$$

$$P_a \approx 453W$$

By comparing the designed well tractor equipment with a standard tractor driller from Qinterra (2015):

Standard driller:

Output torque: 110Nm at 180rpm

$$P(kW) = \frac{T(Nm) \cdot n_{rpm}(rpm)}{9550}$$

$$P(kW) = \frac{110Nm \cdot 180}{9550}$$

$$P(kW) = 2,073kW$$

With a reduction of 40% in shear forces the needed power is 1240W. Adding the extra power needed for the actuator gives 1693W. The effect of ultrasonic vibration gives a reduction of 380W. This power can be used to increase the range or to speed up the drilling process.

4.2.6 Drill Bit

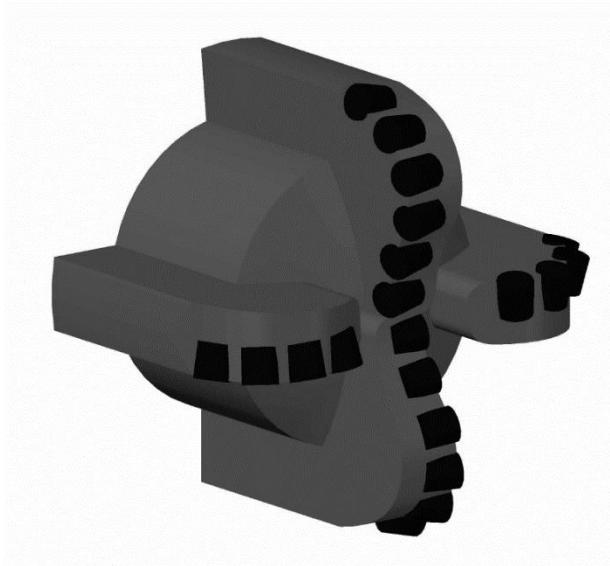


Figure 4.27: Drill bit.

The drill bit (Figure 4.27) is a standard Polycrystalline diamond compact (PDC) bit. Wolfram carbide was chosen as material because the calculations indicated that the extra weight docent have a large influence on the vibration. Wolfram carbide is the normal material to use on PDC bits because of its extreme toughness.

5 Discussion

A discussion of the results are presented in this chapter. The discussion follows the same thematic structure and order as the previous chapter, 4.

5.1 Force Reduction by Vibration

The PPA60L will only be used up to 2000Hz and is by definition not ultrasonic (ultrasonic is defined greater than 20kHz). The low speed compared with other UAD examples, implies that the frequency can be much lower and still have more strokes per mm. The ultrasonic definition is used since it is the industry standard for high frequency assisted drilling.

All samples showed a clear improvement with ultrasonic vibration, especially around 1000Hz and 32 μ m displacement of the cutter. However, as the frequency and displacement measurement during the tests were based on the signal output of the frequency transformer, and not measurements done to the cutting head, the output vibration might be different from the input signal. The actuator in the test rig needs to vibrate a plate in addition to the cutting head, and the mass of the plate and cutting tool could have influenced the actuator. Alternatively, the plate could have flexed, losing some of the movement. This means that the optimum frequency might be slightly lower than 1000Hz and the displacement slightly lower than 32 μ m. It was tried to fit an accelerometer to the test rig, but the accelerometer did not manage to pick up all the movements, so it was rejected. A good alternative could have been a magnetic sensor that can measure both frequency and displacement. For this project, there were no time to order a magnetic sensor when the accelerometer failed.

The test performed on Berea sandstone is the most reliable. From Figure 4.3 you can see that each test, follows the same pattern. The tests on Grunnes soapstone and Dionysos marble shows larger deviations. For the soapstone test something must have disturbed the normal force calibration, as positive numbers should not be possible. Why there were so large variations in the soapstone test is a bit unclear, but it could have been variations in the rock sample. The rock sample was just one piece of soapstone, and not a sample dedicated for testing. For the marble you can see there are some sections where the curve flattens out in Figure 4.7. These flat sections are a result of the rig getting stuck while doing scratch tests in marble.

The speed and amplitude tests performed on Berea sandstone are representative tests. According to the amplitude test it is interesting to look at higher amplitudes.

5.2 Stick-Slip reduction by Vibration

The performed tests did not manage to reproduce a real stick slip. What was obtained from the test was that vibration generally gives a smaller stick. The jagged curve in Figure 4.10 can indicate that vibration counteracts the bit to get really stuck. Rather giving a constant flow of small stick-slips.

5.3 Vibration Effect on Wear

The tests on Berea sandstone is the most representative ones, performed without any interference. On tests performed in marble, the rig got stuck as with the force test in marble.

In addition, the cutter blade just floated on top of the rock sample during the first test, so the scratch needed to be run two times. This happened for both the standard test and the vibration test, and was therefore included in the result.

How representative this test is compared to drill bits where the teeth are made from Polycrystalline diamond compact (PDC) (not steel) is questionable. PDC is built up from industrial diamonds, giving them an extreme hardness. As presented in section 2.1.2 Chang and Bone (2005) also had a problem with wear on softer drilling bits.

5.4 Ultrasonic Assisted Tractor Operation

Piezoelectric actuators are prone to small volume changes because the polarization field in the crystal is not 100% in one direction. If this is the case, it could be a problem; the actuator then needs to push the corresponding volume of high pressure liquid. It is unknown if vacuum bobbles forming when using the actuator is a problem.

If the piezoelectric material is heated above the Curie point, it will get depolarized. It is recommended to only operate at half of the Curie point (Technologies 2015). Well tractors have a maximum temperature of 177°C (Qinterra 2015). The Curie point for PZT-4 is 328°C (Morgan 2010). This means that the temperature for the actuator is close to maximum, and if the voltage transformer, actuator and the electric motor produces any extensive heat, it could be a problem.

A wireline with a small control wire inside could make it possible to control parameters like motor speed, frequency and the amplitude.

6 Conclusion

Conclusions from the experiments:

- The force readings from all the experiments show that ultrasonic vibration has a positive effect on drilling performance in rock samples. Tests performed in Berea sandstone shows 40% and 90% reduction in shear force and normal force respectively.
- Increased speed on the cutter blade indicates a reduction in the effect of ultrasonic vibration in terms of force reduction.
- Increased amplitude indicates improved performance.
- The lack of being able to reproduce any real stick-slips makes it difficult to draw a conclusion if the ultrasonic vibration has any effect on stick-slip.
- The wear test indicates that the ultrasonic vibration has a negative impact in terms of wear on the cutter. More work needs to be done to clarify if this is a problem using Polycrystalline diamond compact (PDC) bits.

The technical drawing shows a solution for integrating a piezoelectric actuator into a tractor driller. The suggested design is feasible. But it should be further investigated if volume change and temperature (discussed in chapter 5.4) will affect the performance.

In general, the results from the force tests are positive and further work should be performed.

7 Proposed Further Work

- Investigation of the temperature and volume. Questions raised in chapter 5.4.
- Run tests with larger amplitudes.
- Scale up the force test using a full size PDC drill bit for scale removal, and investigate the effect of increased drill speed/penetration.
- Perform a new stick slip test. A solution for making a laboratory stick-slip might be to run the test over two different rock samples by placing them close to each other. Then the blade might get stuck in the transition.
- Perform a new wear test with PDC blades. This test needs to be longer than the test performed in the project in order to see the effect of wear on the PDC cutter blade. By installing an actuator on the tool holder of a lathe could be a possible solution.
- Investigate the possibility to introduce ultrasonic vibration to conventional drilling. Investigate the possibility to use a mud motor to generate electric power or wired drill string (NOV 2015).

8 Nomenclature

A = Cross section area of the actuator (m^2)
 C = PZT actuator capacitance (F)
 E = Young's modulus for the PZT compound (Pa)
 f = Operating frequency (Hz)
 F = Force (mass times gravity) (N)
 F_0 = Resonant frequency (Hz)
 $F_{Drill\ bit}$ = Gravity force drill bit (N)
 F_{max} = Block force (N)
 k_{PZT} = PZT actuator stiffness (N/m)
 k_{spring} = Spring stiffness (N/m)
 l = Actuator length (m)
 m_{eff} = Effective mass (kg)
 m_{PZT} = Weight of the actuator(kg)
 m = Mass of end pieces (kg)
 n = number of layers
 n_{rpm} = rounds per minute
 P_a = Average power (W)
 P_{LOST} = Power lost in cable
 R = Resistance (Ω)
 R_a = Resistance in steel armor (Ω)
 R_c = Resistance in copper conductor (Ω)
 T = Torque (Nm)
 U_{LOST} = Voltage lost in cable (V)
 U_{p-p} = Peak-peak drive voltage (V)
 U_{max} = Maximum output voltage swing of the amplifier (V)
 ΔL_0 = Max. nominal displacement without external force (m)
 ΔL_N = Zero point offset (m)
 ΔL_R = Lost displacement due to external spring (m)
 ϵ_{33} = Relative dielectric constant
 ρ_{PZT} = density of PZT-4 (kg/m^3)

9 References

- AkerSolutions. 2014. Wireline tractor and tractor applications, product catalogue.,
<http://www.akersolutions.com/Global/Subsurface/Traktor%20katalog%20August%202013.pdf> (downloaded 20.10 2014).
- Alcona.com. 2015. Infinitofocus for form and roughness measurement,
<http://www.alicona.com/home/products/infinitefocus.html>
(downloaded 12.05 2015).
- Azarhoushang, B., J. Akbari. 2006. Ultrasonic-assisted drilling of Inconel 738-LC (in *International Journal of Machine Tools & Manufacture*).
- Bar-Cohen, Y., S. Sherrit, X. Bao. 2007. Ultrasonic/Sonic Driller/Corer (USDC) as a Subsurface Sampler and Lab-on-a-Drill for Planetary Exploration Applications
- BP. 2010. *Deepwater Oil Spill - Problems with the LMRP cap* (Reprint).
- Chang, Simon S. F., Gary M. Bone. 2005. Burr size reduction in drilling by ultrasonic assistance (in *Robotics and Computer-Integrated Manufacturing* **21** (4-5): 442-450).
- Chen, S. L., K. Blackwood, E. Lamine. 2002. Field Investigation of the Effects of Stick-Slip, Lateral, and Whirl Vibrations on Roller-Cone Bit Performance, Society of Petroleum Engineers (2002/3/1/).
- Cleave, D. V. . 1976. Ultrasonics get bigger jobs in machining and welding (in *Iron age* 69-72).
- Crabtree, Mike, David Eslinger, Phill Fletcher et al. 1999. Fighting Scale - Removal and Prevention (in *Oilfield review*: 30-35).
- Deen, Aron, Ryan Wedel, Abhijeet Nayan. 2011. Application of a Torsional Impact Hammer to Improve Drilling Efficiency (in.
- Edelen, David A. . 2007. System and Method for the Pooling of Sterile Product. doctor, Texas at Arlington.
- Ford, Robert. 2012. Optimized drillbit design cuts cost, time (in *Offshore, World Trends and Technology for Offshore Oil and Gas Operations*).
- Instrumente, Physik. 2001. *Theory and Applications of Piezo Actuators and PZT NanoPositioning Systems* (Reprint).
<http://sites.poli.usp.br/d/pmr5222/apostpiez.pdf>.
- Instrumente, Physik. 2015. Piezo Design: Fundamentals of Piezoelectric Actuation,
[http://www.piezo.ws/piezoelectric actuator tutorial/Piezo Design part3.php](http://www.piezo.ws/piezoelectric%20actuator%20tutorial/Piezo%20Design%20part3.php) (downloaded 21.05 2015).

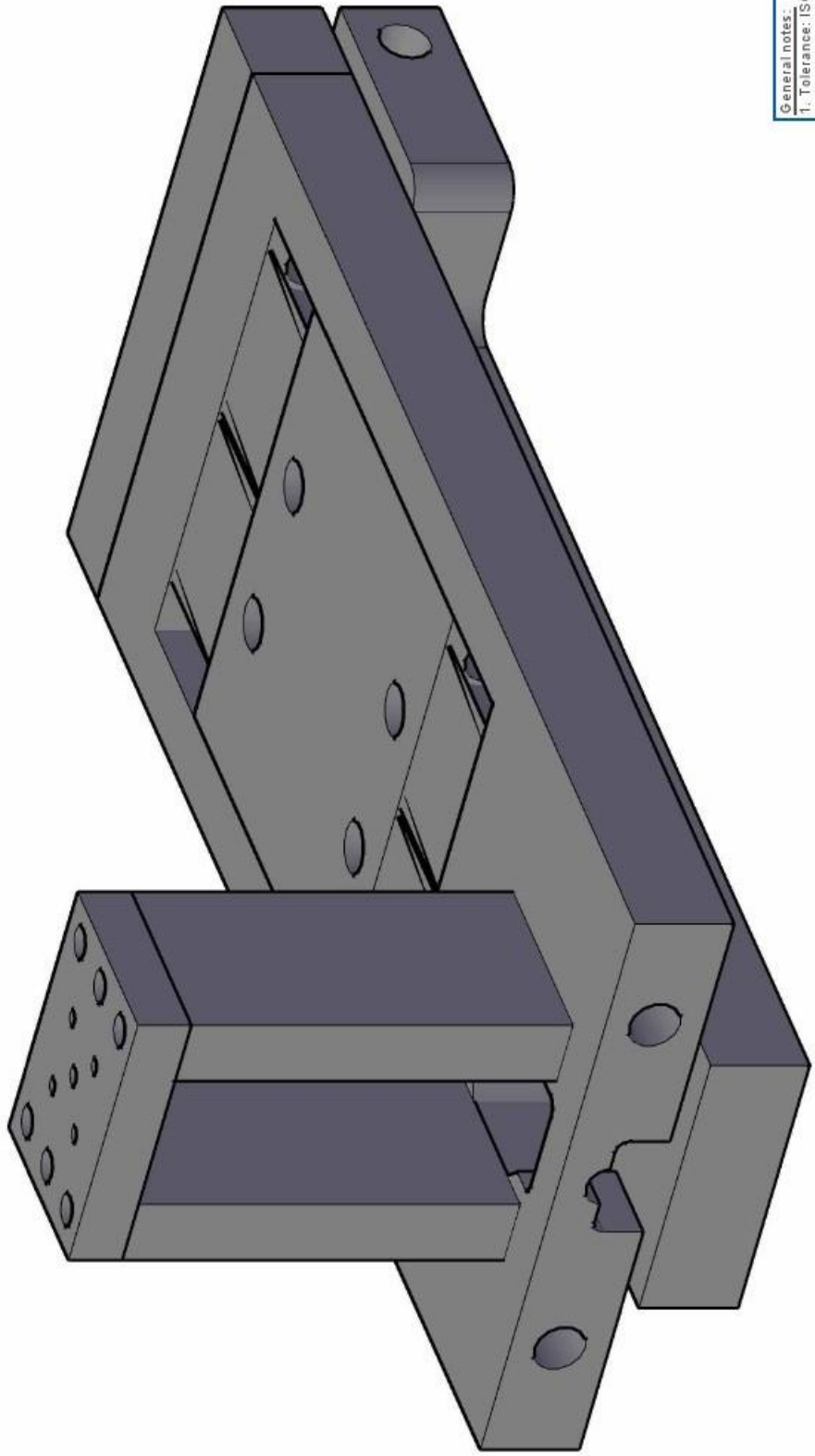
- Ishikawa, Ken-ichi, Hitoshi Suwabe, Tetsuhiro Nishide et al. 1998. A study on combined vibration drilling by ultrasonic and low-frequency vibrations for hard and brittle materials (in **22** (4): 196-205.
- Lu, Eric, Jessie Jin. Planetary gear, https://www.cs.berkeley.edu/~sequin/CS285/2011_REPORTS/CS285%20final%20paper_Eric&Jessie.pdf.
- M4Sciences. What is Piezo?, <http://my.brainshark.com/What-is-a-Piezo-857005951>.
- Mineralszone. Physical Properties of Granite, <http://www.mineralszone.com/stones/sandstone.html>.
- Morgan. 2010. *Properties of piezoelectricity ceramics* (Reprint). <http://www.morgantechnicalceramics.com/sites/default/files/documents/tp226.pdf>.
- Noliac. 2014. *Piezo Actuators* (Reprint). <http://materials.dk/links/D13x4%20Piezo%20aktuatorer.pdf>.
- E-001, Electrical systems. 2001: NORSOK.
- NOV. Wired drill string, [https://www.nov.com/Segments/Wellbore Technologies/IntelliServ/Service and Equipment Delivery.aspx](https://www.nov.com/Segments/Wellbore_Technologies/IntelliServ/Service_and_Equipment_Delivery.aspx).
- Oiltools, Neo. Electric Tractor, <http://www.neo-oiltools.com/applications/electric-tractor>.
- PI. Piezo Mechanisms & Piezo Mechanic Systems for Precision Motion Applications (Mechatronics), <http://www.piezo.ws/index.php#PIEZ>.
- Prabhakar, D. . 1992. Machining Advanced Ceramic Materials Using Rotary Ultrasonic Machining Process.
- Pujana, J., A. Rivero, A. Celaya et al. 2009. Analysis of ultrasonic-assisted drilling of Ti6Al4V (in *International Journal of Machine Tools and Manufacture* **49** (6): 500-508.
- Qinterra. PowerTrac® Advance™ 318, PowerTrack® Direct Drive Rotation, <http://www.qinterra.com/products/wireline-tractor-tools/powertrac-advance-318>, <http://www.qinterra.com/products/rotational-tools/powertrac-direct-drive-rotation>.
- Technologies, Cedrat. 2012. *Cedrat technologies piezo products catalog version 4.1* (Reprint). http://www.cedrat-technologies.com/download/CEDRAT_TEC_Catalogue.pdf.
- Technologies, Piezo. Technical Resource Paper, <http://www.piezotechnologies.com/resources/white-papers/usage-temperatures-of-piezoceramic-materials.aspx>.
- Technology, Piezo. Forces and Stiffnesses, <http://piceramic.com/piezo-technology/properties-piezo-actuators/forces-stiffnesses.html>.

- Tsuboi, Ranko , Yasuhiro Kakinuma, Tojiro Aoyama et al. 2012. Ultrasonic Vibration and Cavitation-aided Micromachining of Hard and Brittle Materials (in *Procedia CIRP* **1** (0): 342-346.
- Wedel, Ryan , Shaun Mathison, Greg Hightower. 2011. Mitigating Bit-Related Stick-Slip With A Torsional Impact Hammer.

Appendix A

Technical drawings

REV:	DESCRIPTION:	BY:	DATE:
0	Contruccion	NV	15.12.14



General notes:
 1. Tolerance: ISO 2768-f
 2. All sharp edges to be rounded R=0,2

SITE:

Ultrasonic assisted drilling test rig

TITLE:

Contruccion

15.12.2014

DATE

PROJECT NO.

CHECKED.

1/2-0/7

SCALE AT AA. DRAWN

1:1

NV

0

REVISION



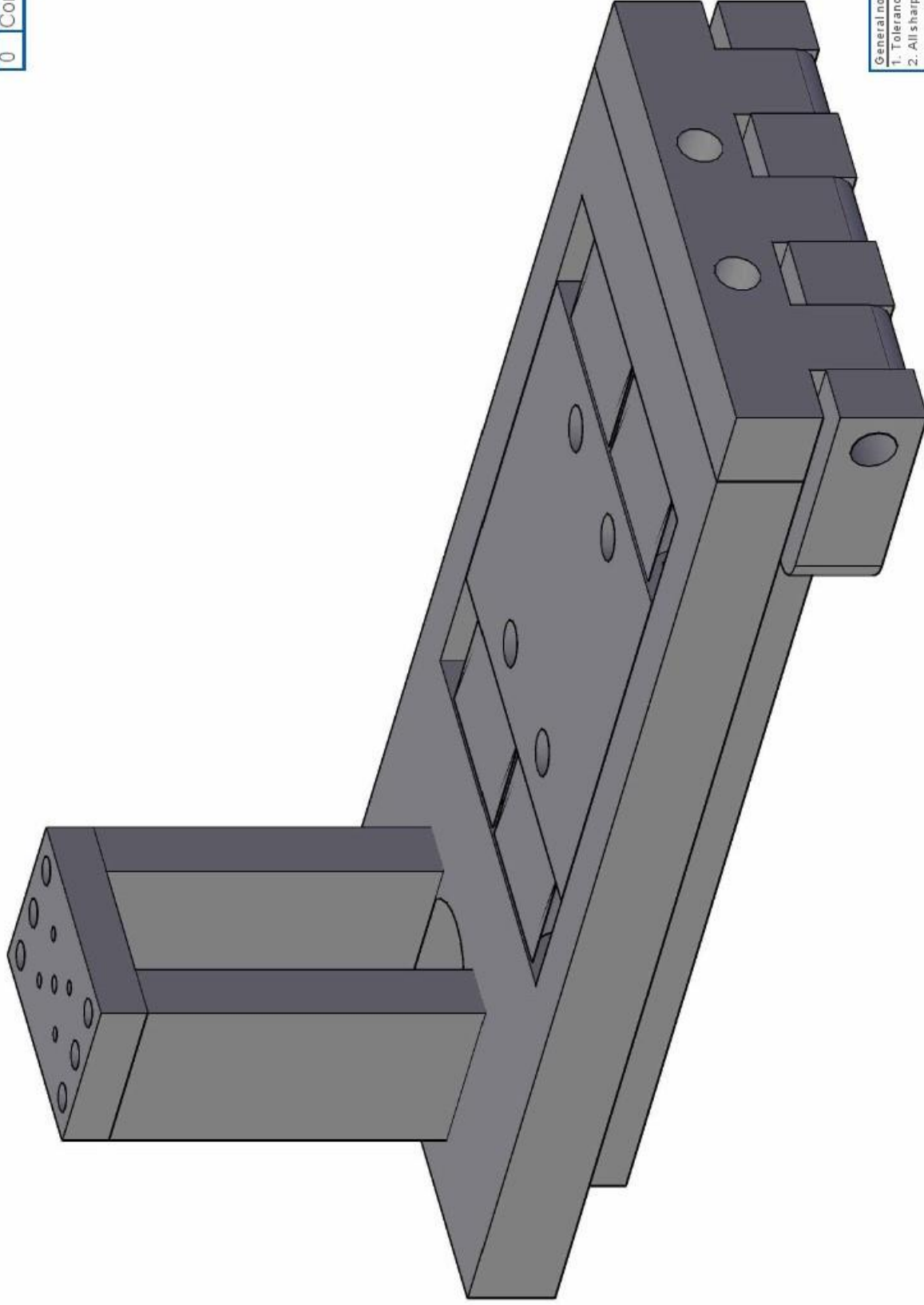
NTNU - IPT

7491 Trondheim

Telephone: 73594925

www.ntnu.no

REV:	DESCRIPTION:	BY:	DATE:
0	Contraction	NV	15.12.14



General notes:

1. Tolerance: ISO 2768-f
2. All sharp edges to be rounded R=0.2

SITE:

Ultrasonic assisted drilling test rig

TITLE:

Contraction

15.12.2014

DATE:

PROJECT NO.

2/2-0/7

DRAWING NO.

1:1

SCALE AT AA.

NV

DRAWN.

0

REVISION.

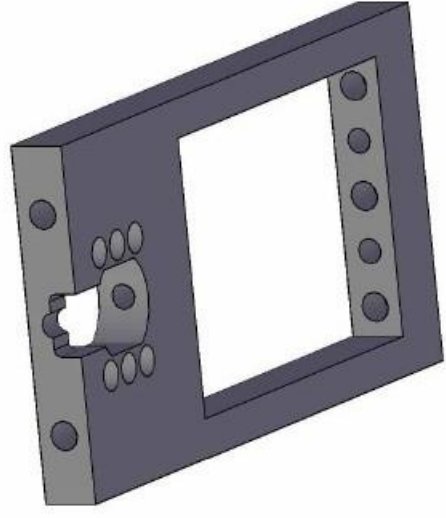
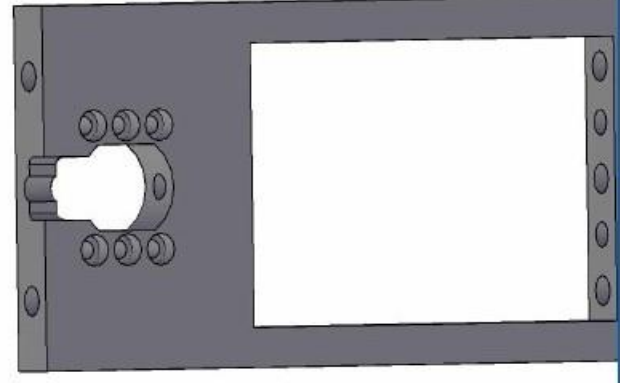
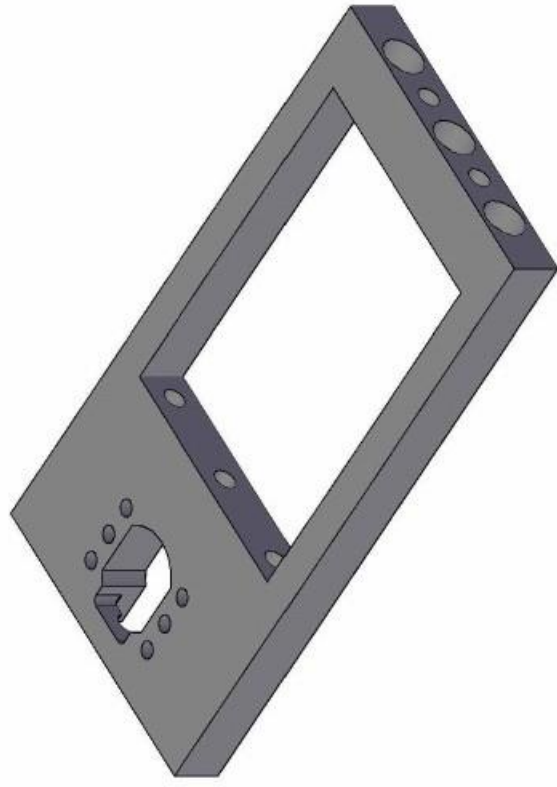
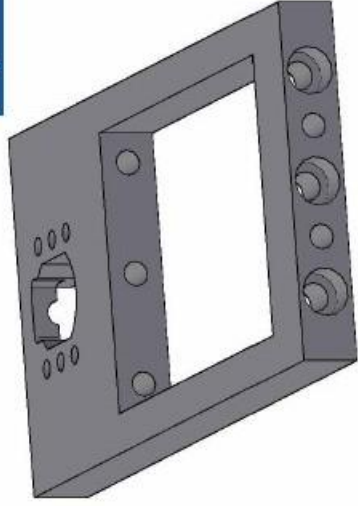
CHECKED.

NTNU - IPT

7491 Trondheim
Telephone: 73594925
www.ntnu.no



REV:	DESCRIPTION:	BY:	DATE:
0	Contraction	NV	15.12.14

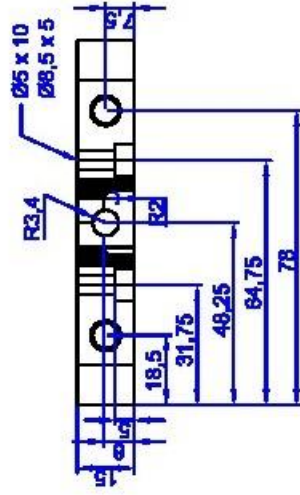
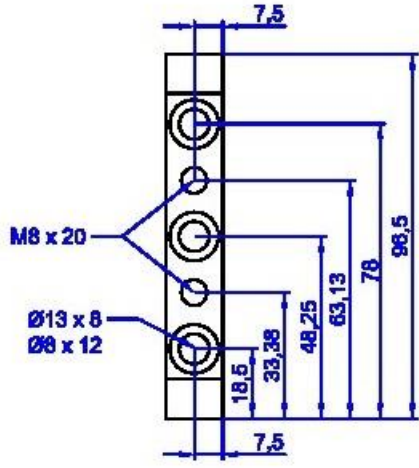


General notes:
 1. Tolerance: ISO 2768-f
 2. All sharp edges to be rounded R=0.2

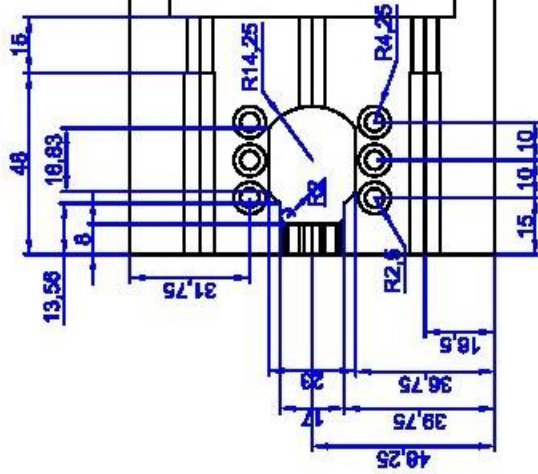
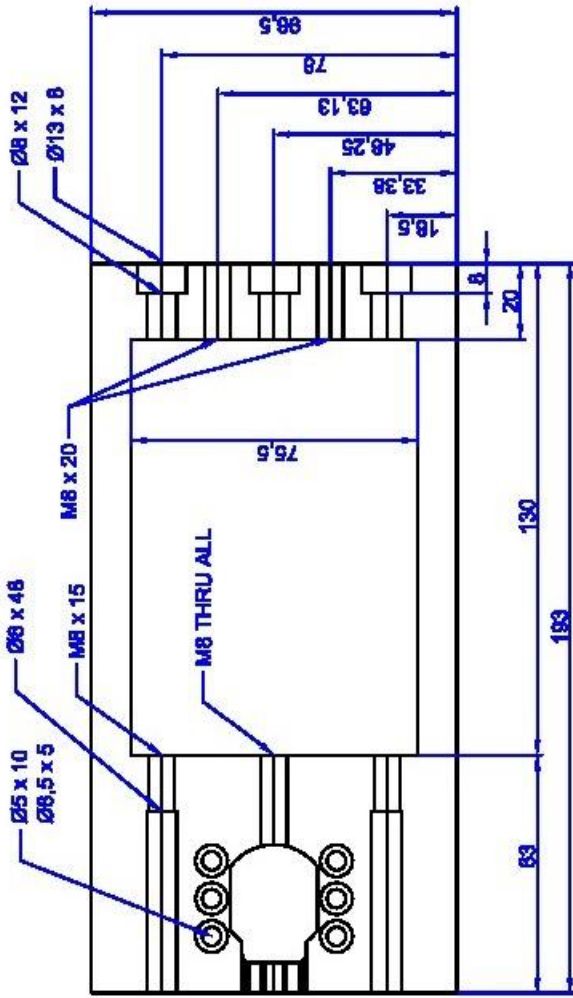
SITE: NTNU - IPT	PROJECT NO. 15.12.2014		DATE 15.12.2014
	SCALE AT AA. 1:2	DRAWING NO. 1/2-1/7	REVISION 0
TITLE: Base plate	CHECKED.		REVISION 0
NTNU - IPT 7491 Trondheim Telephone: 73594925 www.ntnu.no			



REV:	DESCRIPTION:	BY:	DATE:
0	Contraction	NV	15.12.14



General notes:
 1. Tolerance: ISO 2768-f
 2. All sharp edges to be rounded R=0.2



NTNU - IPT
 7491 Trondheim
 Telephone: 73594925
 www.ntnu.no

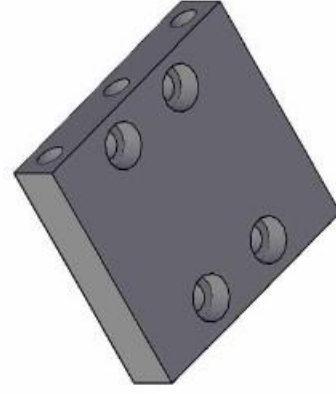
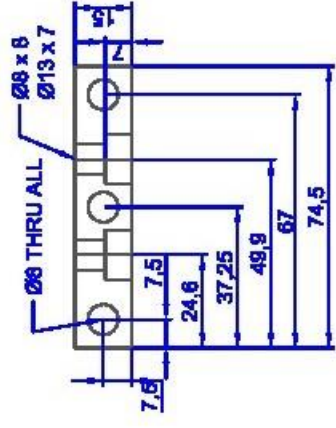
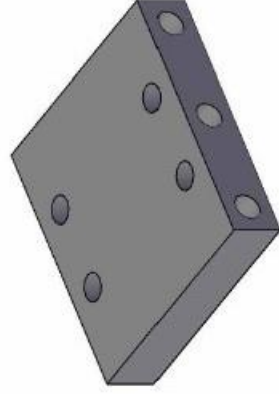
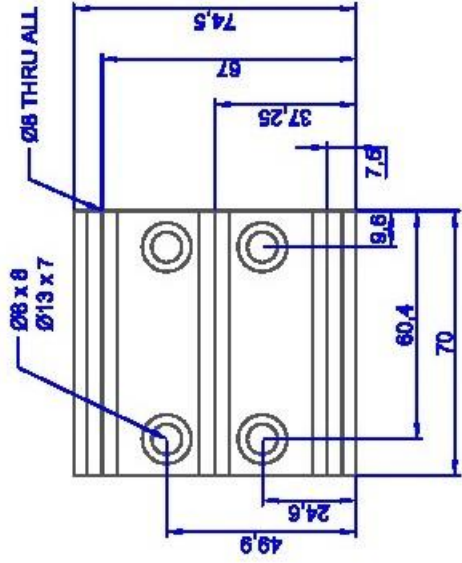


15.12.2014	PROJECT NO.	CHECKED.	REVISION
DATE			
			0

1/2-1/7	DRAWING NO.	NV
1:2	SCALE AT A4	DRAWN

SITE: Ultrasonic assisted drilling test rig
 TITLE: Base plate

REV:	DESCRIPTION:	BY:	DATE:
0	Construction	NV	15.12.14



General notes:
 1. Tolerance: ISO 2768-f
 2. All sharp edges to be rounded R=0.2

SITE: Ultrasonic assisted drilling test rig

TITLE: Slide mount

DRAWING NO. 1/1-2/7

SCALE AT AA. 1:2
 DRAWN. NV

PROJECT NO. 15.12.2014

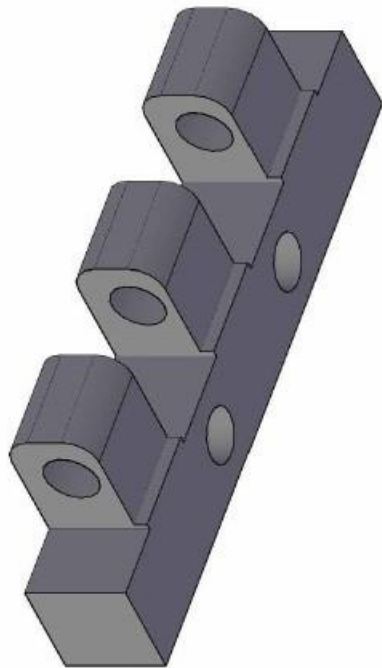
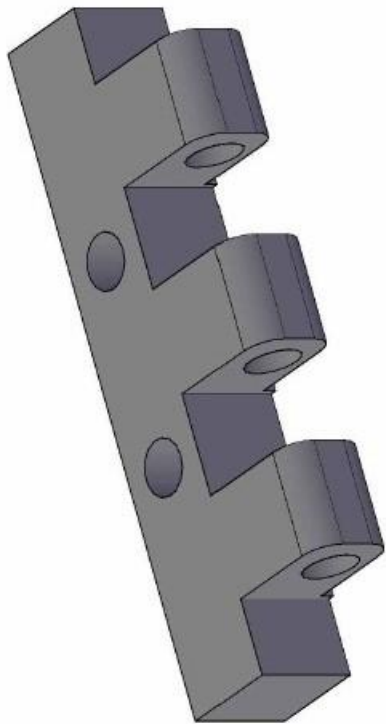
DATE 15.12.2014
 REVISION 0

NTNU - IPT



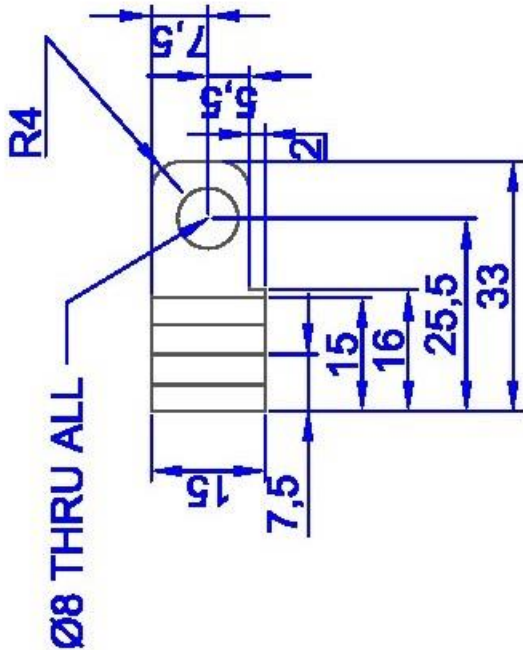
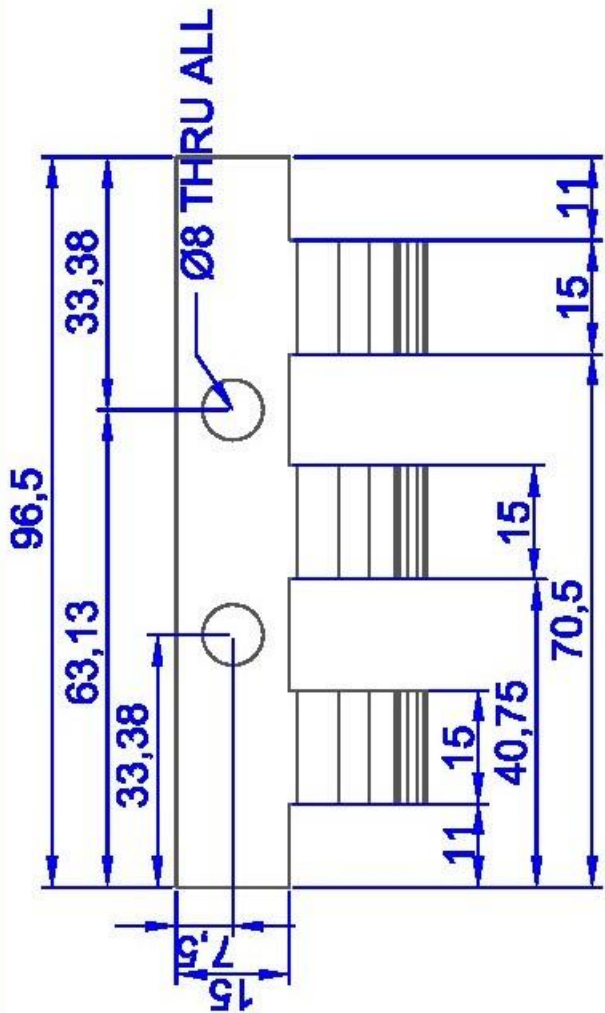
7491 Trondheim
 Telephone: 73594925
 www.ntnu.no

REV:	DESCRIPTION:	BY:	DATE:
0	Contruccion	NV	15.12.14



General notes:

1. Tolerance: ISO 2768-f
2. All sharp edges to be rounded R=0.2



SITE:

Ultrasonic assisted drilling test rig

TITLE:

Hinge

1/1-3/7

DRAWING NO.

1:1

SCALE AT A4.

NV

DRAWN.

PROJECT NO.

CHECKED.

15.12.2014

DATE

0

REVISION



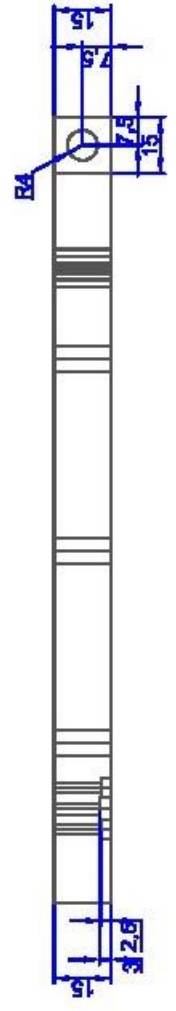
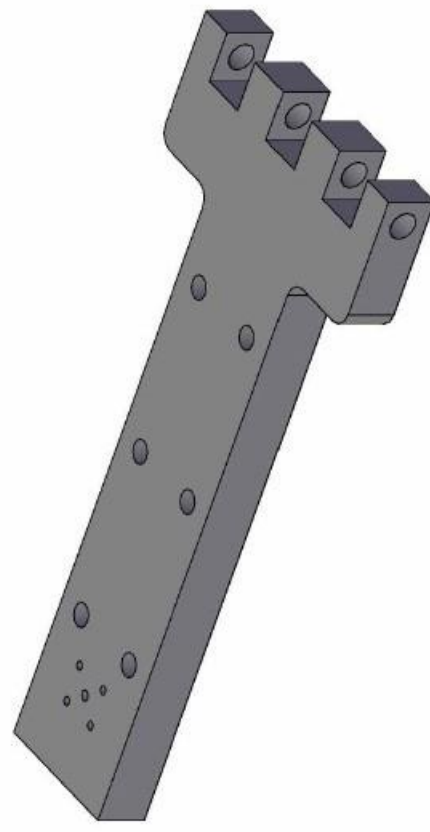
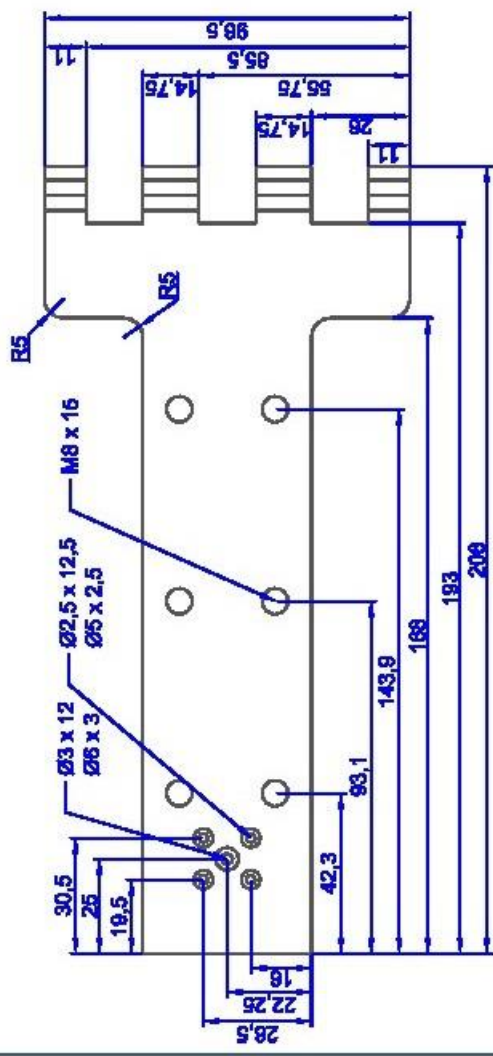
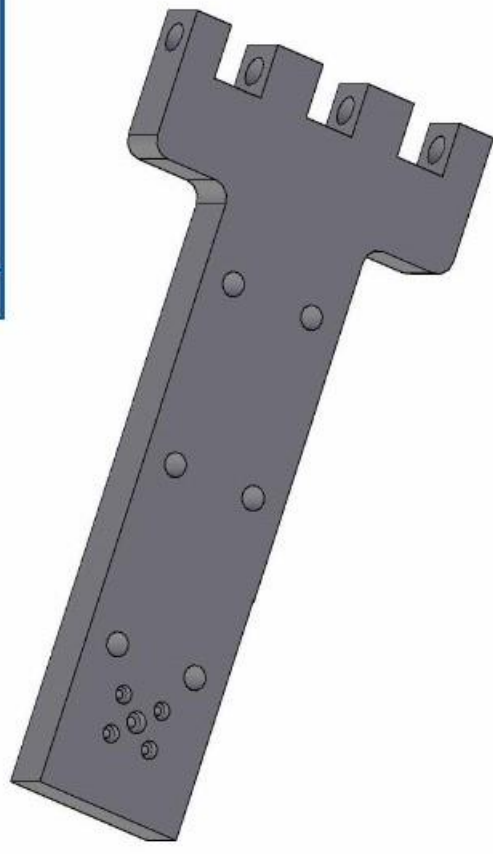
NTNU - IPT

7491 Trondheim

Telephone: 73594925

www.ntnu.no

REV:	DESCRIPTION:	BY:	DATE:
0	Construction	NV	15.12.14



General notes:

1. Tolerance: ISO 2768-f
2. All sharp edges to be rounded R=0,2

SITE:

Ultrasonic assisted drilling test rig

1/1-4/7

DRAWING NO.

15.12.2014

DATE

NTNU - IPT

7491 Trondheim

Telephone: 73594925

www.ntnu.no



1:2

SCALE AT A4

Vibrating plate

TITLE:

NV

DRAWN

CHECKED

REVISION

0

PROJECT NO.

15.12.2014

DATE

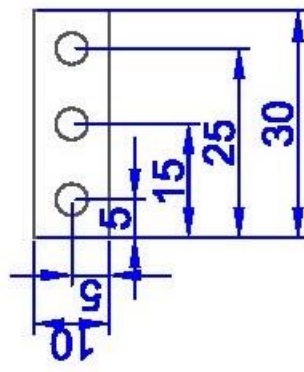
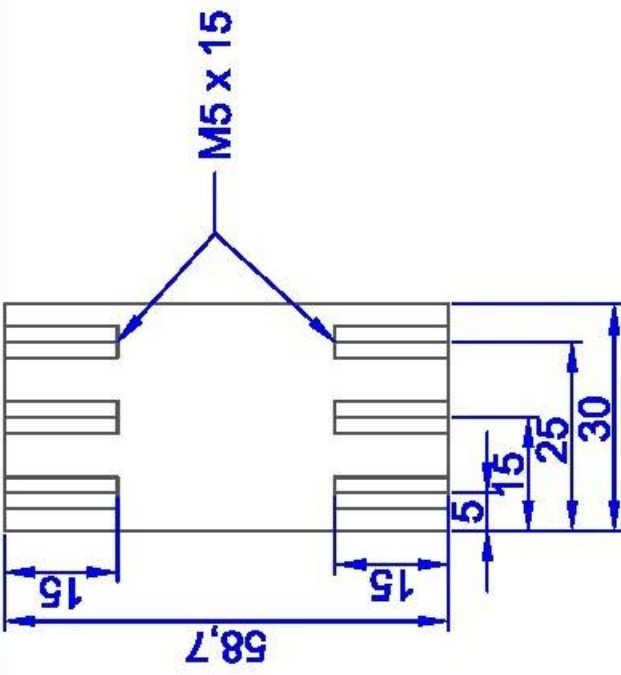
15.12.2014

DATE

15.12.2014

DATE

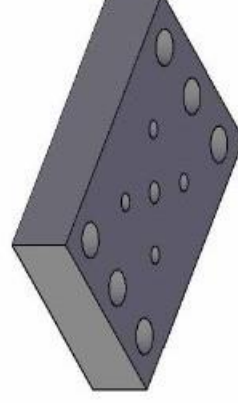
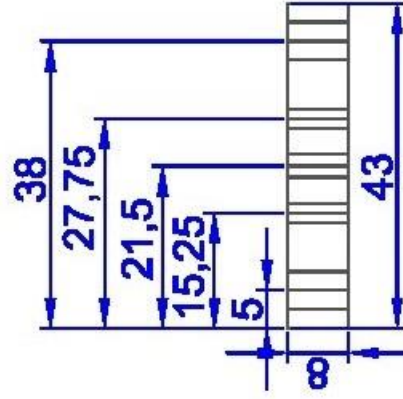
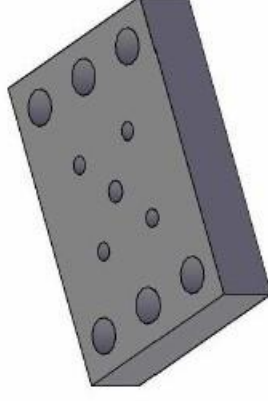
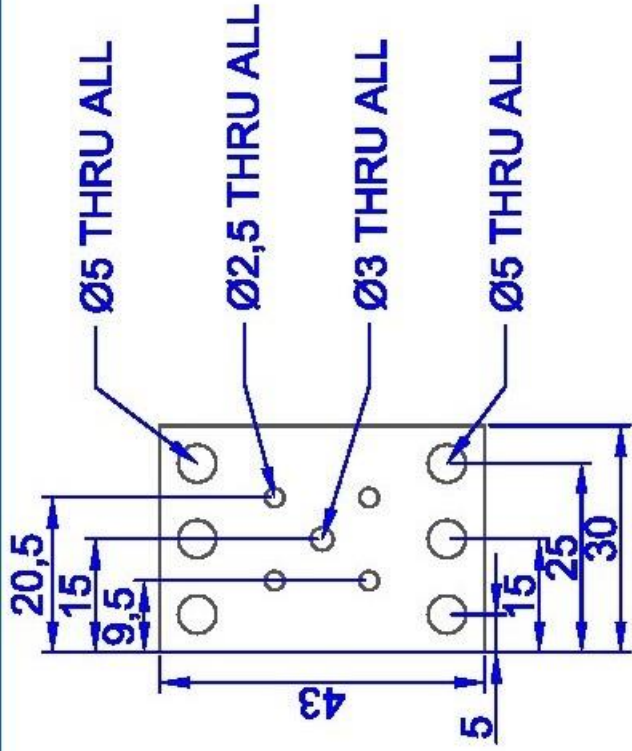
REV:	DESCRIPTION:	BY:	DATE:
0	Construction	NV	15.12.14



General notes:
 1. Tolerance: ISO 2768-f
 2. All sharp edges to be rounded R=0,2

SITE:	Ultrasound assisted drilling test rig		DRAWING NO.	1/1-5/7	PROJECT NO.	15.12.2014	NTNU - IPT 7491 Trondheim Telephone: 73594925 www.ntnu.no			
	TITLE:	Tower pillar		x2		SCALE AT A4:		1:1	CHECKED:	

REV:	DESCRIPTION:	BY:	DATE:
0	Construction	NV	15.12.14



General notes:

1. Tolerance: ISO 2768-f
2. All sharp edges to be rounded R=0,2

SITE:

Ultrasound assisted drilling test rig

DRAWING NO. 1/1-6/7

15.12.2014
DATE

NTNU - IPT



7491 Trondheim
Telephone: 73594925
www.ntnu.no

TITLE:

Hinge

SCALE AT A4. 1:1

NV

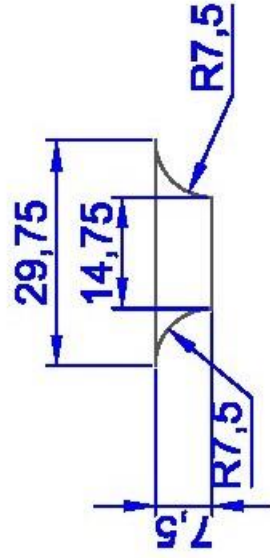
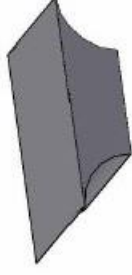
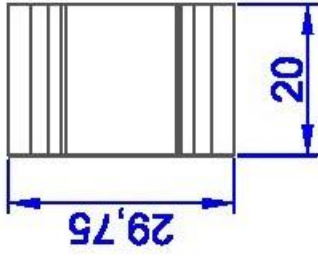
0

REVISION

CHECKED.

DRAWN.

REV:	DESCRIPTION:	BY:	DATE:
0	Contraction	NV	15.12.14



General notes:

1. Tolerance: ISO 2768-f
2. All sharp edges to be rounded R=0,2

SITE:

Ultrasonic assisted drilling test rig

DRAWING NO.
1/1-7/7

15.12.2014
DATE

NTNU - IPT



7491 Trondheim
Telephone: 73594925
www.ntnu.no

TITLE:

Lock tool x4

SCALE AT AA.
1:1

DRAWN.
NV

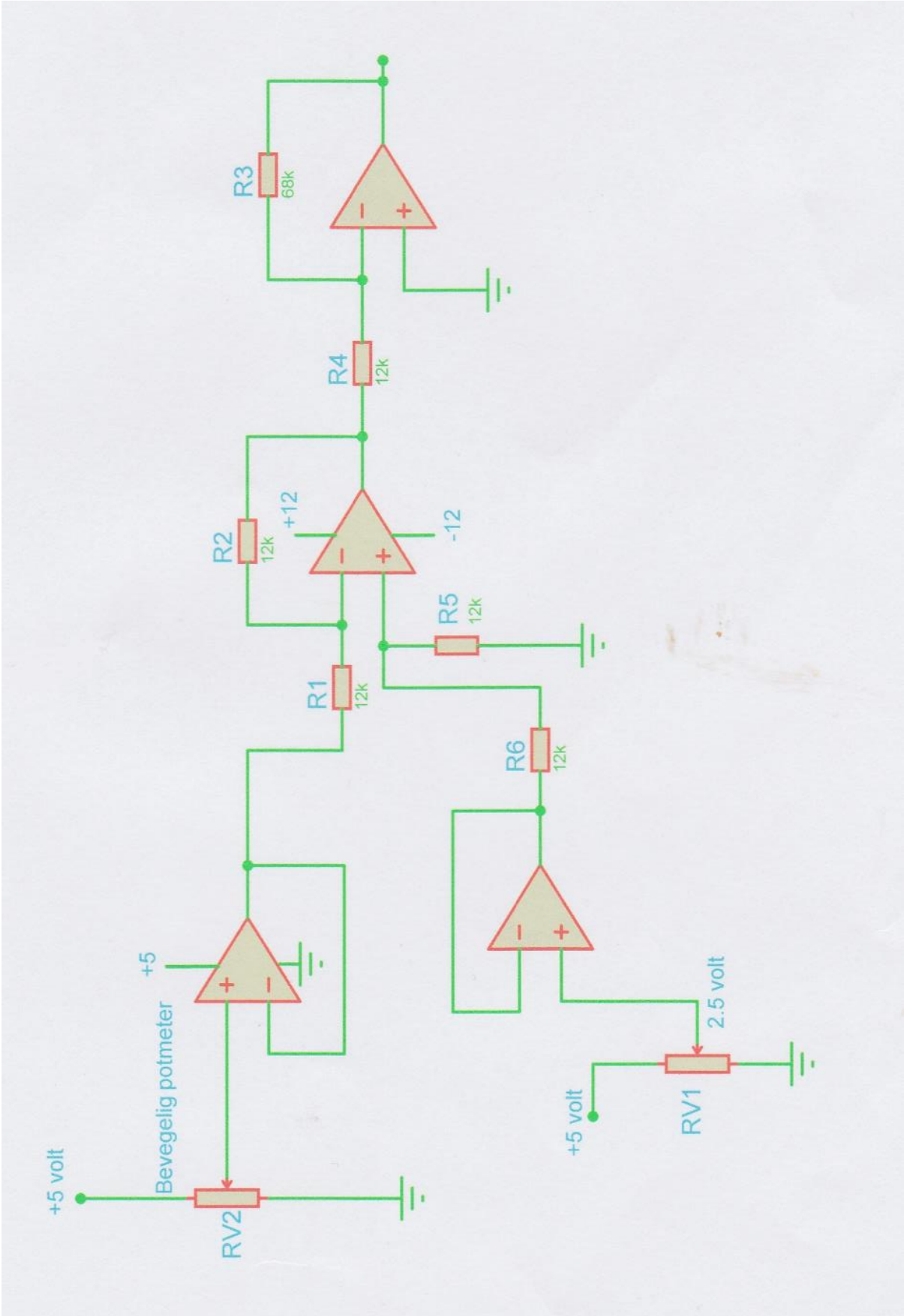
PROJECT NO.

CHECKED.

REVISION
0

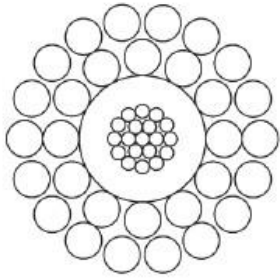
Appendix B

Electric circuit for processing potentiometer signal



Appendix C

Wireline



**7/16" (10.80 mm)
MONOCONDUCTOR, LOW RESISTANCE
1N42 – LR**

PROPERTIES

Cable Diameter	0.425" +0.006" - 0.002"	(10.80mm + 0.15mm - 0.05mm)
Minimum Sheave Diameter	24"	(61 cm)
Cable Stretch Coefficient	0.70 ft/Kft/Klbs	(0.79 m/Km/5KN)

ELECTRICAL

Maximum Conductor Voltage	1,500 VDC	
Conductor AWG Rating	13	
Minimum Insulation Resistance	1,500 Mega Ω /Kft @ 500VDC	(457 Mega Ω /Km @ 500VDC)
Armor Electrical Resistance	1.2 Ω /Kft	(3.94 Ω /Km)

MECHANICAL

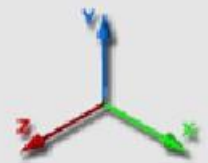
Cable Breaking Strength			
Ends Fixed	19,500 lbs	(86.8 KN)	Nominal
Maximum Suggested Working Tension	9,750 lbs	(43.4 KN)	
Number and Size of Wires			
Inner Armor	12 x 0.0585"	(1.490 mm)	
Outer Armor	18 x 0.0585"	(1.490 mm)	
Average Wire Breaking Strength			
Inner Armor	765 lbs	(3.4 KN)	
Outer Armor	765 lbs	(3.4 KN)	

Cable Type	Core Description							Cable Weight	
	Temp Rating °F °C	Plastic Type	Insulation Thickness in mm	Copper Construction in mm	Res Typical Ω /Kft Ω /Km	Cap. Typical pf/ft pf/m	O.D. Each in mm	in Air	in H ₂ O
								lbs/Kft Kg/Km	
1N42PTZ-LR	500 260	FEP	0.0255	19x0.0172	2.0 6.6	37.5 123	0.136	336 499	278 413
		ETFE	0.648	19x0.437			3.454		
			0.035				0.206		
		0.890		5.232					

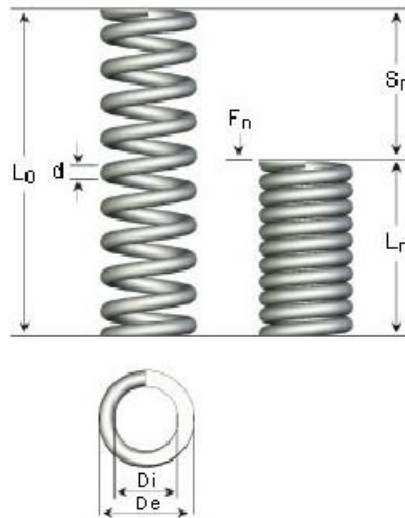
- The armor wires are high tensile, Galvanized Extra Improved Plow Steel (GEIPS), and coated with anti-corrosion compound for protection during shipping and storing. Wires are preformed.
- Core assembly – Copper strand consists of a total of nineteen wires. Conductor resistance is measured at 68° F. Voids in the copper strand are filled with a water-blocking agent to reduce water and gas migration.
- SUPERSEAL, a special pressure seal agent, is applied between armor layers.
- The temperature rating assumes a normal gradient for both temperature and weight.
- All values shown are nominal or typical values.

Appendix D

Springs



Trykfjedre Serie A Piano tråd Ø2,00 - Ø3,20



Lagernummer

13190

Benævnelse

Compression Spring A 13190



Materiale	DIN 17223 C wire W. nr. 1.1200
d Tråd	2.80
De Udvendig diameter	14.00
Di Indvendig diameter	8.40
L0 Fri længde.	20.50
Ln Maks belastet længde	16.40
sn Max Vandring	4.10
Dd Max Aksel	7.80
Dh Min Hul	14.60
n Fjedrende vindinger	3.50
Fn Max kraft	518.77
R Konstant N/mm	127.49
Afslutning	Closed and ground

Created: 2015-05-11 19:34:49

Address:

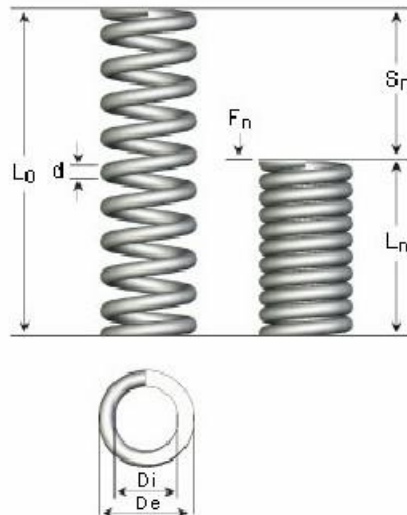
Sodemann Industrifjedre A/S
Industrivej 21
DK-8260 VIBY J
Denmark

Phone:
Fax:
Web:

0045 86 72 00 99
0045 86 29 97 86
www.fjedre.dk, www.fjadrar.se, www.jouset.com,
www.fjaer.net, www.industrial-springs.com



Trykfjedre Serie B Piano tråd Ø1,73 - Ø2,67



Lagernummer

C04800721000M

Benævnelse

Compression Spring B C04800721000M



Materiale	DIN 17223 C wire W. nr. 1.1200
d Tråd	1.83
De Udvendig diameter	12.19
Di Indvendig diameter	8.53
L0 Fri længde.	25.40
Ln Maks belastet længde	17.65
sn Max Vandring	7.75
nt vindinger Kun vejledende	5.40
Fn Max kraft	144.47
R Konstant N/mm	18.61
Afslutning	Closed and ground

Address:

Sodemann Industrifjedre A/S
Industrivej 21
DK-8260 VIBY J
Denmark

Phone:
Fax:
Web:

0045 86 72 00 99
0045 86 29 97 86
www.fjedre.dk, www.fjadrar.se, www.jouset.com,
www.fjaer.net, www.industrial-springs.com

Appendix E

Piezoelectric actuator, PPA60L

TABLE OF STANDARD PROPERTIES OF USE AND MEASUREMENT

The properties defined in the table below, are set up according to the technical conditions of use and measurement. These properties are warranted within their variation range and in compliance with the standard technical conditions of use.

Properties PPA60L	Standard technical conditions	Unit	Nominal values	Min. values	Max. values
Notes		-	-	-	-
Max. no load displacement	Quasistatic excitation, blocked-free	µm	60	54	69
Blocked force	Quasistatic excitation, blocked-free	N	3500	2800	4200
Stiffness	Quasistatic excitation, blocked-free	N/µm	58,33	46,67	64,17
Resonance frequency (free-free)	Harmonic excitation, free-free, on the admittance curve	Hz	9500	8075	11400
Response time (free-free)	Harmonic excitation, free-free, on the admittance curve	ms	0,05	0,05	0,06
Capacitance	Quasistatic excitation, free-free, on the admittance curve	µF	20,00	18,00	26,00
Max. tensile force	Static effort, blocked-free	N	1750	1313	1750
Resolution	Quasistatic excitation	nm	0,60	-	-
Height (in actuation direction)		mm	77,00	76,80	77,20
Depth (base)		mm	23,50	23,40	23,60
Width (base incl. wedge & wires)		mm	18,00	17,90	18,10
Mass		g	117,0	-	-
Standard mechanical interface (top)	1 centered M3 threaded hole 5 mm deep & 4 M2.5 threaded holes on Ø 15 mm 4 mm deep	-	-	-	-
Standard mechanical interface (base)	1 centered M3 threaded hole 5 mm deep & 4 M2.5 threaded holes on Ø 15 mm 4 mm deep	-	-	-	-
Standard electrical interface	2 PTFE insulated AWG26 wires 100 mm long with Ø 1 banana plug	-	-	-	-

PROPERTIES STANDARD TECHNICAL CONDITIONS OF USE AND MEASUREMENT

Free-free	: The actuator is not fixed
Blocked-free	: The actuator is fixed to a mechanical support assumed infinitely stiff
Quasistatic excitation	: AC voltage between -20 and 150 V at 1 Hz
Harmonic excitation	: Voltage of 0.5 Vrms, sinusoidal mode from 0 to 100 kHz
Max. harmonic excitation	: Voltage defined by the measurement of max. displacement, sinus at resonance frequency
Displacement measurement	: Laser interferometer, capacitive displacement sensor
Admittance measurement	: HP 4194 A or Cypher C60 electrical impedance analyser
Environment	: Ambient temperature (15-25°C) and dry air (Humidity < 50 % rH)

Any technical conditions of use, different from those defined above, can lead to temporary or definitive alterations of properties. Thank you to contact CEDRAT TECHNOLOGIES before using actuators under non standard technical conditions.

FACTORY TESTS CARRIED OUT

- Test 1 : Electrical admittance vs. Frequency, free-free
- Test 2 : Displacement vs. input voltage

EXTRA FACTORY TESTS

- Test 3 : Gain and linearity of the sensor
- Test 4 : Step response in closed loop
- Test 5 : Stability in closed loop

MECHANICAL INTERFACE

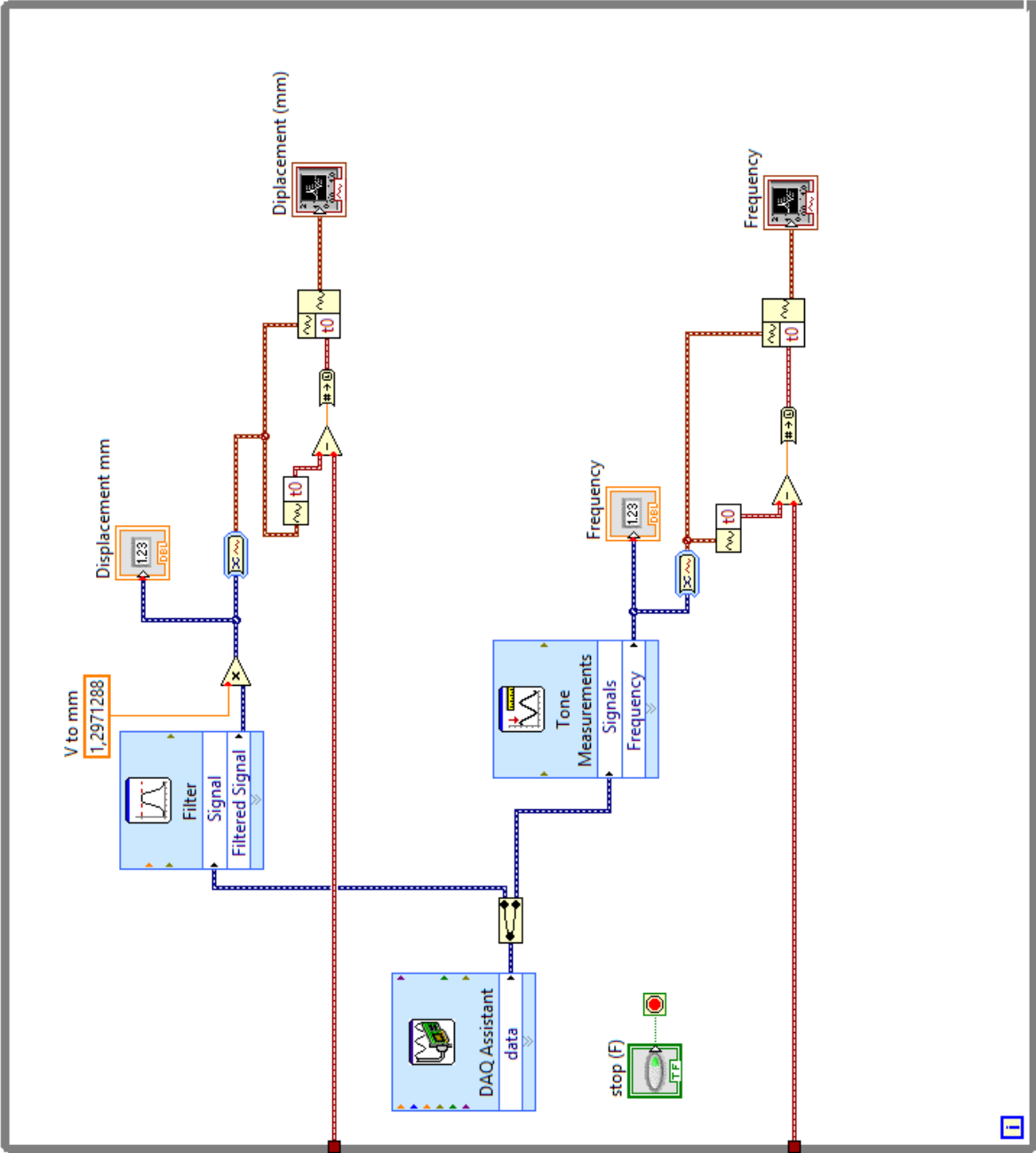
- | | | |
|--|---|--|
| <input type="checkbox"/> [FI] Flat Interface | <input type="checkbox"/> [H] Flat Interface with hole | <input checked="" type="checkbox"/> [TH] Flat Interface with threaded hole |
| <input type="checkbox"/> [SV] Specific version | <input type="checkbox"/> [FF] Free-free Interface | <input checked="" type="checkbox"/> [SI] Specific interface |

AVAILABLE OPTIONS

- | | | |
|--|---|---|
| <input checked="" type="checkbox"/> [SG] Strain gauges | <input type="checkbox"/> [ECS] Eddy current displacement sensor | <input type="checkbox"/> [NM] Non-magnetic sensor |
| <input checked="" type="checkbox"/> [VAC] Vacuum | | |

Appendix F

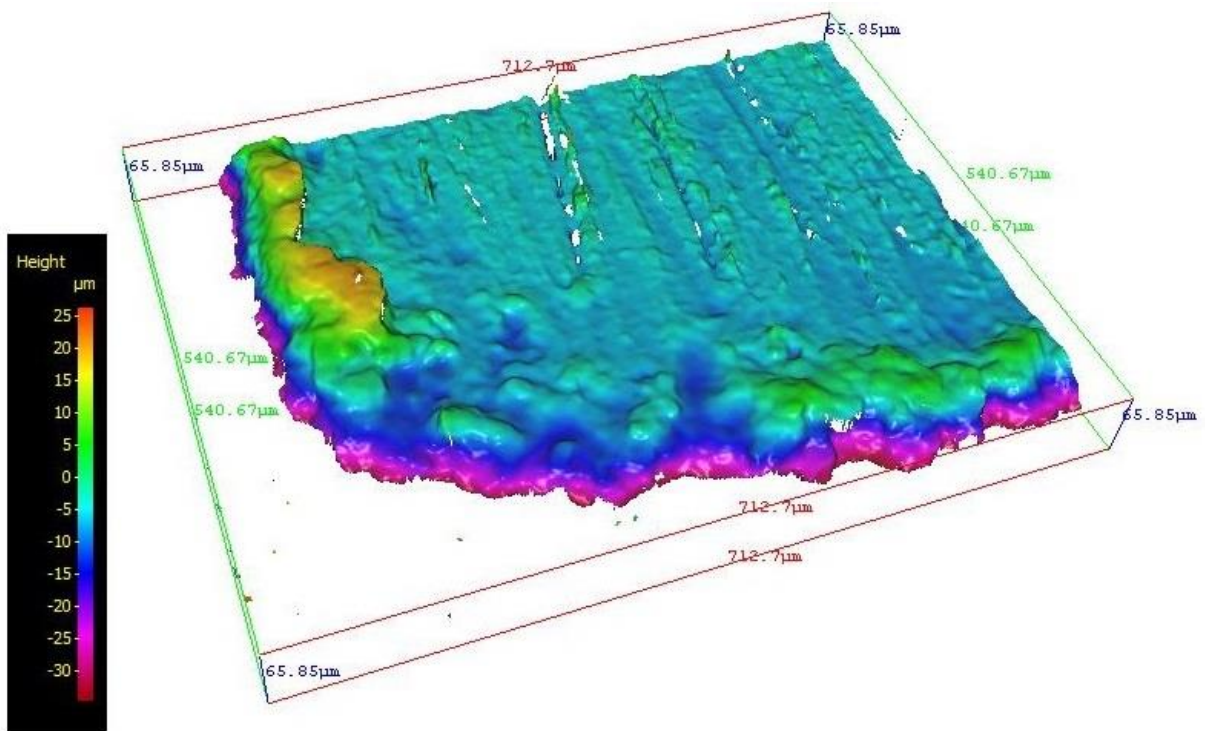
LabView program



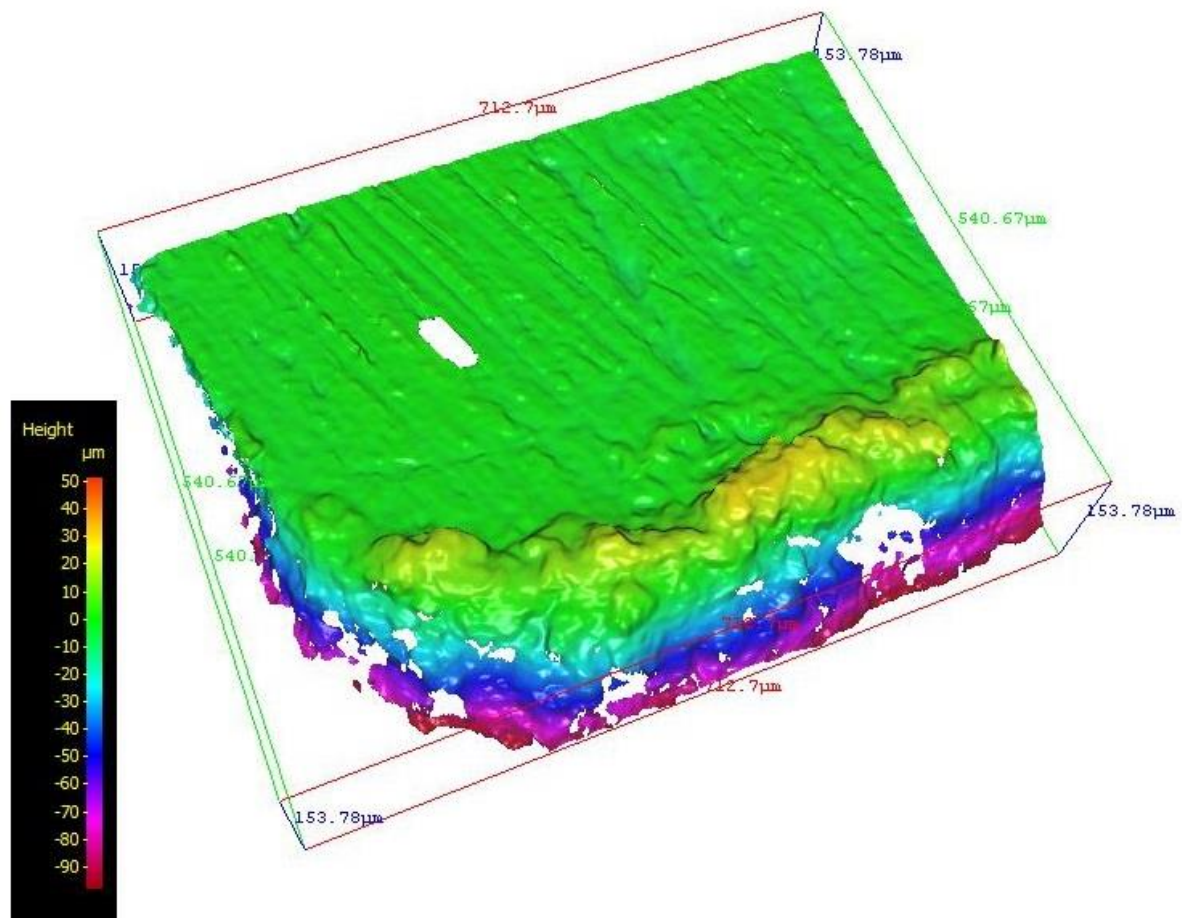
Appendix G

3D pictures with profile indication

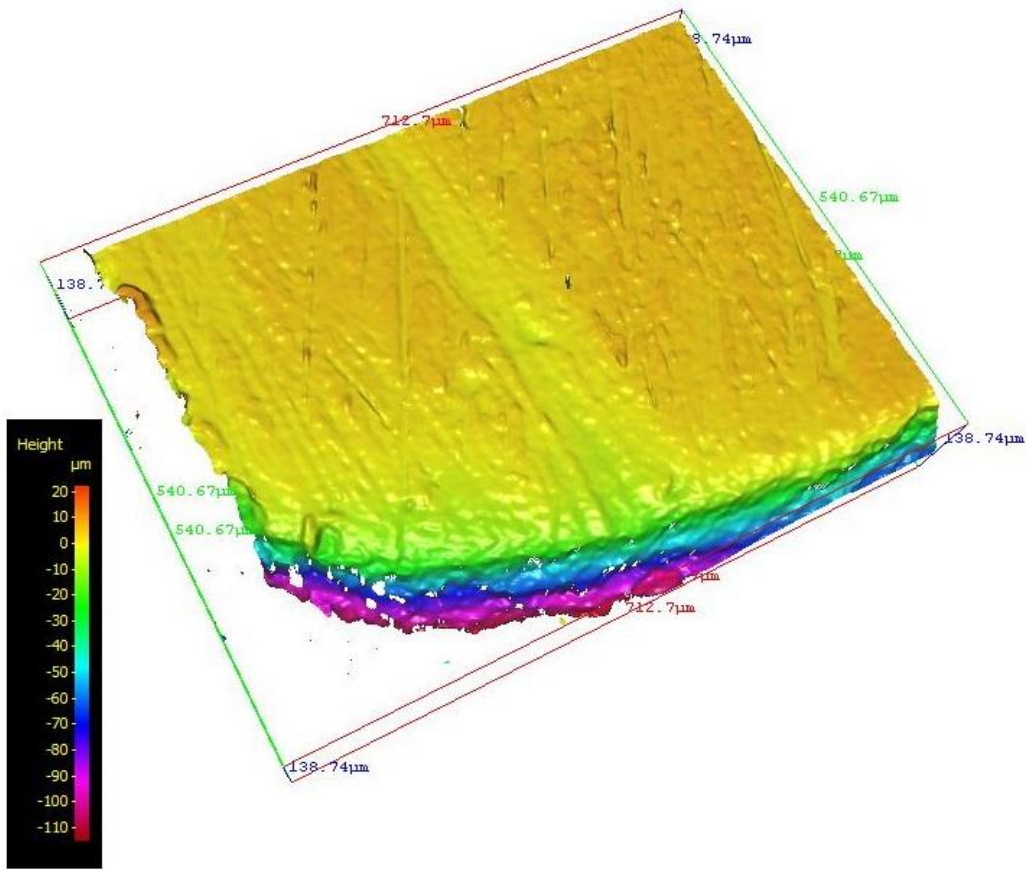
0Hz Berea sandstone:



1000Hz Berea sandstone:



0Hz Dionysos Marble:



1000Hz Dionysos Marble:

